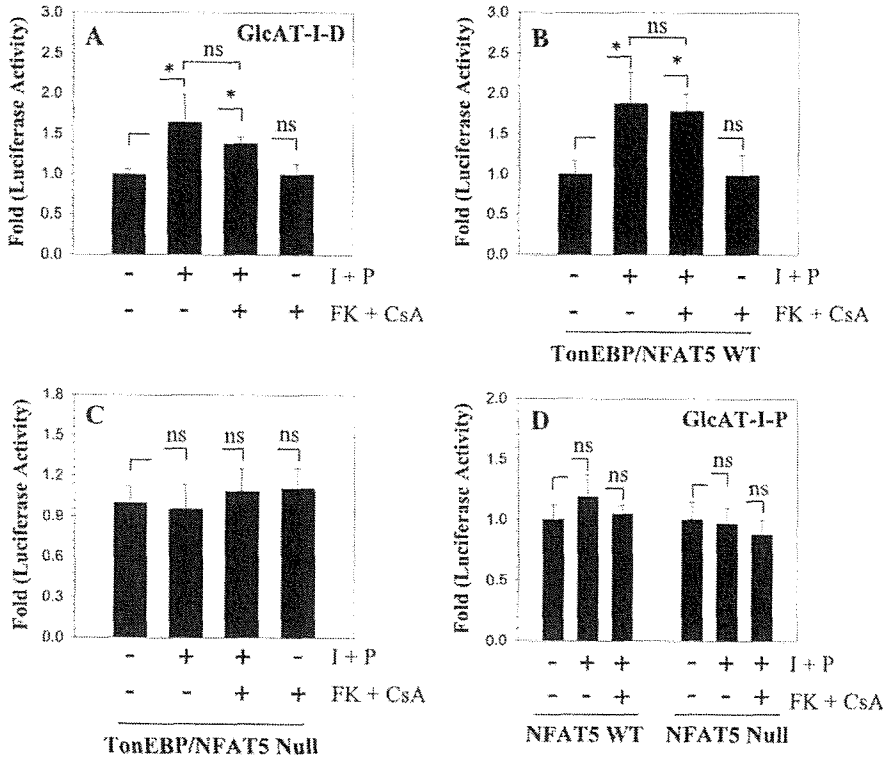


FIGURE 6. **Ionomycin mediates GlcAT-I promoter activation, although TonEBP is independent of calcineurin.** Nucleus pulposus cells (*A*), TonEBP/NFAT5 wild type (*B*), and TonEBP/NFAT5 null (*C*) MEFs were transfected with GlcAT-I-D reporter, and activity was measured following treatment with ionomycin with or without FK506 and cyclosporine A. Unlike TonEBP/NFAT5, null MEFs GlcAT-I-D reporter activity was induced in both nucleus pulposus and NFAT5 wild type cells. Calcineurin inhibitors did not suppress ionomycin-induced or basal activity of GlcAT-I reporter in any of the cell types. *D*, effect of ionomycin treatment on GlcAT-I-P reporter activity. The reporter was nonresponsive to ionomycin treatment in both TonEBP/NFAT5 wild type and null MEFs. Values shown are mean ± S.D. of three independent experiments performed in triplicate. *, $p < 0.05$.

We next examined the effect of ionomycin treatment on GlcAT-I promoter activity in nucleus pulposus cells. When cells are treated with ionomycin and PMA, there is an increase in activity of −1170/+61 bp GlcAT-I promoter (pGlcAT-I-P); the shortest promoter fragment (pGlcAT-I-P), lacking TonE and NFAT sites, did not show any change in activity (Fig. 3*A*). We then determined if ionomycin-mediated activation of GlcAT-I required calcium ions. When cells were treated with the calcium chelator BAPTA-AM along with ionomycin, there was complete inhibition of GlcAT-I-D reporter activation (Fig. 3*B*). To investigate if TonEBP participated in ionomycin-mediated induction of GlcAT-I promoter activity, nucleus pulposus cells were transiently co-transfected with plasmids encoding DN-TonEBP or full-length TonEBP. Fig. 3*C* shows that forced expression of DN-TonEBP completely abolishes ionomycin induction of GlcAT-I promoter activity. Moreover, expression of DN-TonEBP also suppresses the basal activity of the GlcAT-I-D promoter fragment (Fig. 3*D*). A significant inhibitory effect of DN-TonEBP expression on GlcAT-I reporter activity is seen at a dose of 100 ng, which is further enhanced when the concentration of the DN-TonEBP is increased to 400 ng (Fig. 3*D*). On the other hand, overexpression of TonEBP using the pFLAG-TonEBP vector results in a dose-dependent increase in GlcAt-I-D promoter activity in the absence of ionomycin (Fig. 3*E*). We used MEFs derived from TonEBP/NFAT5 null and wild type mice to further validate the role of TonEBP in regulation of the GlcAT-I promoter. Fig. 3*F* shows that the basal GlcAT-I promoter activity in null cells is 50% lower than in the wild type cells. Moreover, co-transfection with TonEBP expression vector in null cells results in an increase in basal GlcAT-I promoter activity (Fig. 3*G*).

We then evaluated whether GlcAT-I promoter activity required that TonEBP be bound to TonE. For this purpose, we introduced a 4-base pair mutation in the TonE site of the GlcAT-I-D reporter plasmid (TTTCCA to TAAAAA). Following ionomycin treatment, nucleus pulposus cells transfected with wild type reporter plasmid evidence induction of activity (Fig. 4*A*). In contrast, when a mutant plasmid is used, induction of the reporter is completely blocked (Fig. 4*A*). Moreover, wild type promoter also exhibited a significantly higher basal activity than the TonE mutant reporter (not shown). We used the ChIP assay to evaluate the interaction of TonEBP protein with the TonE motif in the GlcAT-I promoter (Fig. 4*B*). TonEBP associated with the TonE motif under basal conditions. Binding of TonEBP to TonE was proportional to the amount of transfected FLAG-TonEBP vector. When an empty FLAG vector was co-transfected in place of FLAG-TonEBP, PCR analysis indicated that the amplicon is not formed. This was confirmed by cloning and sequencing of the PCR product.

The mechanism of TonEBP activation by ionomycin in nucleus pulposus cells was investigated. Fig. 5*A* shows that ionomycin treatment results in increased TonEBP mRNA expression. Moreover, both immunofluorescence and Western blot analysis indicate that there is a concomitant increase in TonEBP protein expression (Fig. 5, *B* and *C*); the increase in protein level is evident as early as 8 h, and it remains high at 24 h (Fig. 5*C*). We explored the possibility that activation of Cn, a calcium-dependent phosphatase that mediates NFATc signaling, was responsible for TonEBP induction. Treatment of nucleus pulposus cells with Cn inhibitors, FK506 and cyclosporine A, in the presence of ionomycin did not block induction in TonEBP protein levels (Fig. 5, *B* and *C*). In addition, we measured the promoter activity of the TonEBP target gene, *tauT*. Significant activation in *tauT* reporter activity is evident following ionomycin treatment; simultaneous treatment with Cn inhibitors fails to suppress induction (Fig. 5*D*). In contrast to

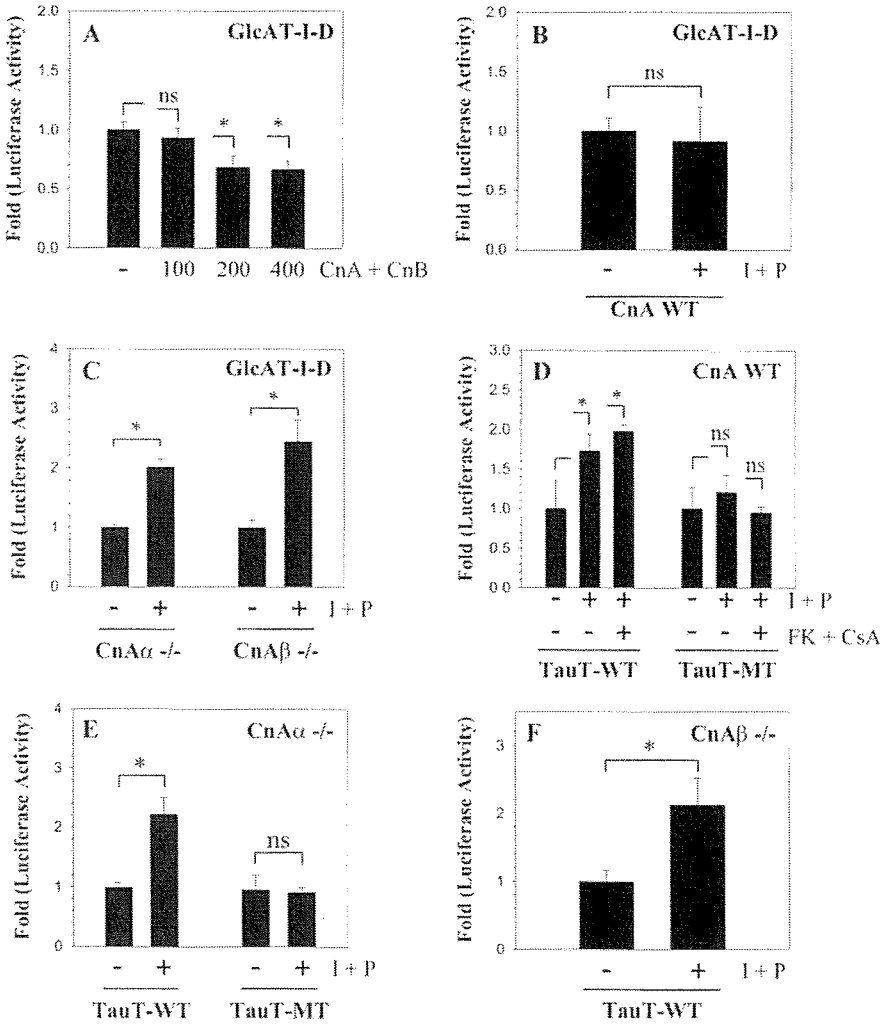


FIGURE 7. **Calcineurin suppresses GlcAT-I promoter function.** *A*, the GlcAT-I reporter activity following co-transfection with calcineurin A/B constructs or empty vector pBJ5 in nucleus pulposus cells. Co-expression of calcineurin subunits suppressed GlcAT-I reporter activity in transfected cells. *B–F*, reporter activity of medullary fibroblasts derived from CnA WT or CnAα or CnAβ null (−/−) mice transfected with GlcAT-I or *tauT* (WT or MT) reporter and treated with ionomycin and PMA with or without FK506 and CsA. Ionomycin did not increase GlcAT-I reporter activity in wild type cells (*B*), but a robust induction was observed in both the CnAα or CnAβ null cells (*C*). A similar high induction in the activity of *tauT*-WT reporter was observed in CnAα or CnAβ null cells; a relatively small inductive effect was seen in wild type cells, which remained constant after the addition of calcineurin inhibitors FK506 and CsA. Neither wild type (*D*) nor the null cells (*E* and *F*) displayed induction in *tauT*-MT reporter activity. Values shown are mean ± S.D. of three independent experiments performed in triplicate. *, $p < 0.05$.

the wild-type *tauT* reporter, activity of mutant *tauT* construct is unaffected by ionomycin (Fig. 5*E*). To confirm that ionomycin promotes Cn-NFAT signaling in nucleus pulposus cells, we measured the activity of 3×NFAT reporter. Fig. 5*F* shows that ionomycin treatment significantly up-regulates 3×NFAT reporter activity, which is completely blocked by the addition of Cn inhibitors FK506 and cyclosporine A.

To ascertain if Cn signaling together with TonEBP plays a role in GlcAT-I expression, we treated nucleus pulposus cells with ionomycin and PMA together with FK506 and cyclosporine A. Fig. 6*A* shows that ionomycin treatment results in an increase in GlcAT-I promoter activity. The presence of FK506 and cyclosporine did not block ionomycin-dependent induction in promoter activity. To further validate these findings, we used NFAT5 null and wild type MEFs and measured activities of GlcAT-I reporters following ionomycin treatment. Fig. 6*B* shows that ionomycin causes an increase in GlcAT-I reporter activity. Again, inclusion of FK506 and cyclosporine did not affect promoter induction in wild type MEFs. In contrast, in NFAT5 null MEFs, ionomycin did not alter GlcAT-I reporter activity (Fig. 6*C*). Moreover, neither wild type nor null cells exhibit an increase in GlcAT-I-P reporter (Fig. 6*D*).

The contribution of Cn signaling in GlcAT-I expression was studied by co-transfecting nucleus pulposus cells with plasmids expressing CnA and CnB along with GlcAT-I-D reporter. Fig. 7*A* shows that nucleus pulposus cells receiving 200 ng or more of Cn plasmids display suppression in GlcAT-I reporter activity. To further explore if Cn signaling played a regulatory role, we used primary medullary fibroblasts derived from CnAα null, CnAβ null, and wild type mice. Treatment of wild type fibroblasts with ionomycin results in little change in GlcAT-I reporter activity (Fig. 7*B*). Interestingly, in both CnAα null and CnAβ null cells, ionomycin treatment enhances activation (2-3-fold) of the GlcAT-I-D reporter (Fig. 7*C*). We then measured the activity of both wild type (containing the WT TonE motif) and mutant *tauT* reporter (mutant TonE motif) in these cells. Wild type cells show a small increase in the activity of the WT-*tauT* reporter; activity is unaffected by the calcineurin inhibitors (Fig. 7*D*). A significant induction in *tauT* reporter is also seen in both CnAα (Fig. 7*E*) and CnAβ (Fig. 7*F*) null cells. Mutant *tauT* reporter is not induced in either the wild type, CnAα, or CnAβ null fibroblasts.

To investigate the relationship between GlcAT-I and NFAT signaling, we transfected nucleus pulposus cells with plasmids encoding NFAT1–4 and measured the activity of the GlcAT-I-D reporter. Fig. 8*A* shows that co-expression of NFAT1 alone has no effect on GlcAT-I reporter activity. However, when Cn (CnA and CnB) was co-expressed with or without NFAT1, there is a significant suppression in reporter activity. Unlike NFAT1, co-expression of CA-NFAT2 (Fig. 8*B*), NFAT3 (Fig. 8*C*), or NFAT4 (Fig.

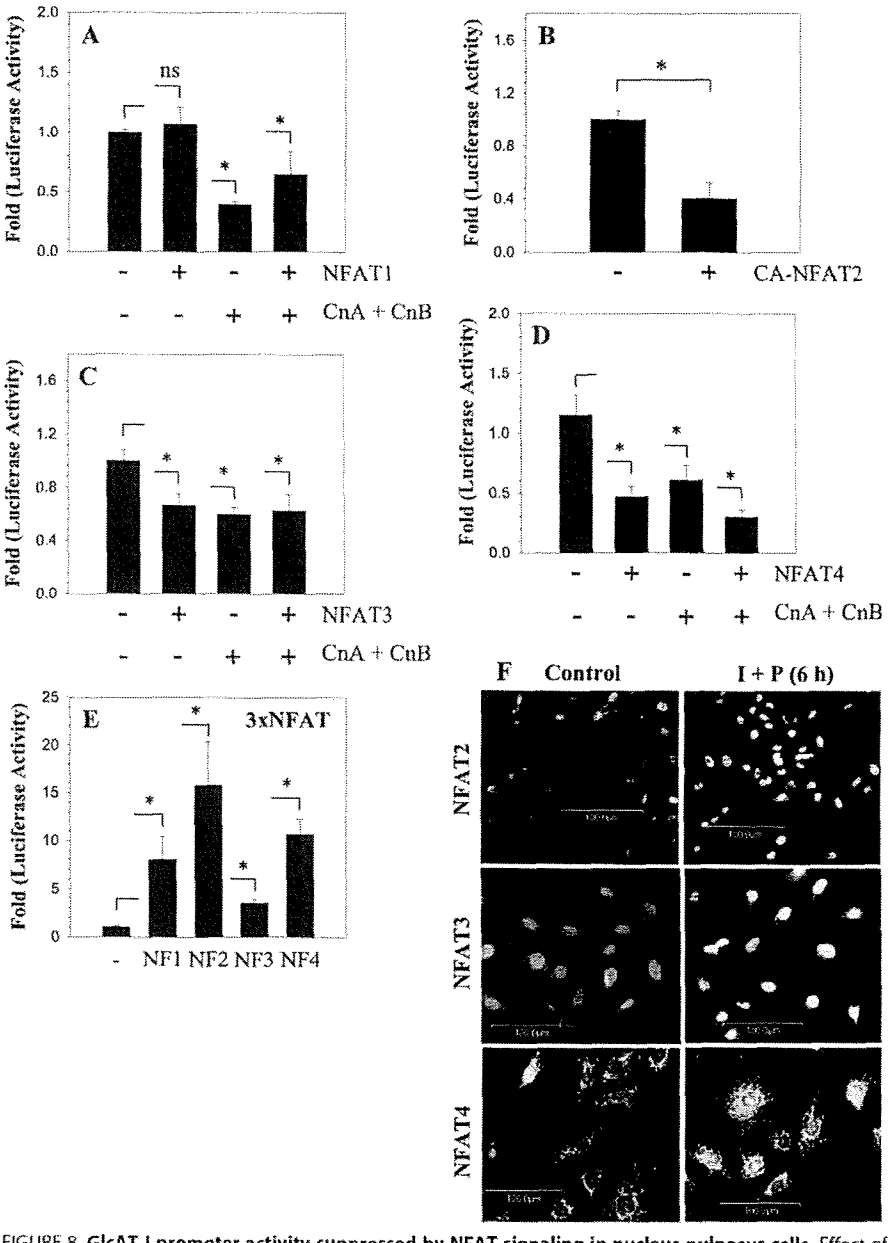


FIGURE 8. **GlcAT-I promoter activity suppressed by NFAT signaling in nucleus pulposus cells.** Effect of NFAT vectors (NFAT1, -2, -3, and -4) and/or CnA and CnB on GlcAT-I-D reporter activity of nucleus pulposus cells. *A*, NFAT1 alone did not affect GlcAT-I reporter activity. When calcineurin was added alone or together with NFAT1, there was a suppression in reporter activity. CA-NFAT2 (*B*), NFAT3 (*C*), or NFAT4 (*D*) alone or when added with CnA/B significantly suppressed the GlcAT-I-D reporter activity in nucleus pulposus cells. *E*, nucleus pulposus cells were transfected with 3×NFAT luciferase construct with or without NFAT1, CA-NFAT2, NFAT3, or NFAT4, and reporter activity was measured. Co-expression of NFAT1 to -4 resulted in a significant increase in activity of 3×NFAT reporter plasmid, indicating functionality of expressed proteins. Values shown are mean ± S.D., of three independent experiments. *, $p < 0.05$; *ns*, nonsignificant. *F*, activation and nuclear localization of NFAT2/3/4 following ionomycin treatment of nucleus pulposus cells.

8*D*), with or without Cn plasmids, suppresses GlcAT-I promoter activity in nucleus pulposus cells. To confirm that transfected NFAT plasmids expressed functional proteins in nucleus pulposus cells, we measured activation of an NFAT-responsive 3×NFAT reporter. Fig. 8*E* shows that there is significant activation of 3×NFAT luciferase reporter when co-transfected with NFAT1 or CA-NFAT2, NFAT3, or NFAT4 expression plasmids. We used immunofluorescence microscopy to confirm expression and activation of endogenous NFAT2, -3, and -4 in rat nucleus pulposus cells. Fig. 8*F* shows that under basal conditions, NFAT2, -3, and -4 are expressed by the nucleus pulposus cells and mostly localize to the cytoplasm. Increased localization of these proteins to nuclei is seen following a 6-h treatment of cells with ionomycin (Fig. 8*F*).

Finally, we investigated if Sp1 activity is required for TonEBP regulation of GlcAT-I promoter function in nucleus pulposus cells. We treated nucleus pulposus cells with WP631, an inhibitor of Sp1 activity, with or without ionomycin and measured the activity of GlcAT-I reporters. Treatment with WP631 at 50–100 nM completely abolishes ionomycin-mediated induction in GlcAT-I-D reporter activity as well as suppressing basal promoter activity (Fig. 9*A*). On the other hand, ionomycin did not induce GlcAT-I-P reporter (−123/+61 bp), and the activity remained unaffected by WP631 (Fig. 9*B*). To further validate these findings, nucleus pulposus cells were co-transfected with plasmid encoding DN-Sp1. Fig. 9*C* shows that expression of DN-Sp1 completely abolishes ionomycin induction of GlcAT-I promoter activity. Moreover, expression of DN-TonEBP also suppresses the basal activity of the GlcAT-I-D promoter fragment (Fig. 9*D*). A significant inhibitory effect of DN-TonEBP expression on GlcAT-I reporter activity is seen at a dose of 100 ng, which is further enhanced when the concentration of the DN-Sp1 is increased to 200 ng (Fig. 9*D*).

## DISCUSSION

The experiments described in this investigation demonstrated for the first time that GlcAT-I, a key enzyme required for chondroitin sulfate biosynthesis, was regulated by TonEBP (NFAT5). This transcription factor would serve to promote the expression of a critical enzyme required for GAG chain synthesis as well as enhancing the expression of the aggrecan core protein (4). Our studies revealed that the regulated expression of GlcAT-I in nucleus pulposus cells was calcium-dependent. This finding is of critical functional importance, since shifts in calcium ions serve as key transducers of

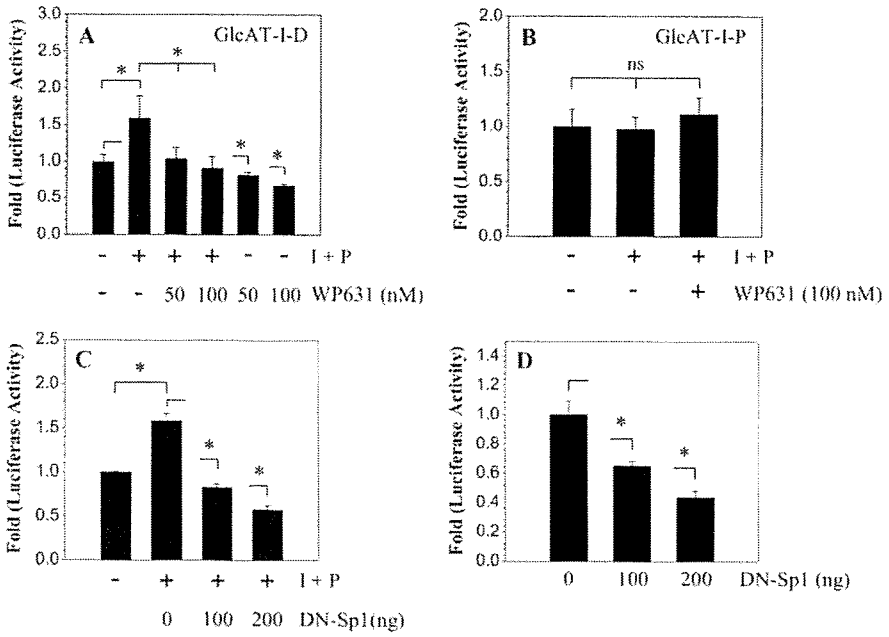


FIGURE 9. **TonEBP and Spl are both required for calcium-mediated regulation of GlcAT-I promoter activation in nucleus pulposus cells.** Cells were transfected with GlcAT-I-D (*A*) or GlcAT-I-P (*B*) promoter constructs and treated with ionomycin with or without WP631 (50–100 nM), an Spl inhibitor. Note that suppression of Spl function resulted in complete loss of ionomycin-mediated induction of GlcAT-I reporter. *B*, ionomycin failed to induce activity of GlcAT-I-P construct lacking the TonE motif in nucleus pulposus cells; WP631 has no effect on the activity of this reporter. Values shown are mean ± S.D. of three independent experiments. *, $p < 0.05$; *ns*, nonsignificant.

applied biomechanical loads. Accordingly, loading would promote calcium flux and enhance the synthesis of hydrated proteoglycans. A second major observation was that members of the NFAT family were expressed by nucleus pulposus cells; in this case, calcium-dependent Cn-NFAT signaling functioned as a negative regulator of GlcAT-1 expression. Thus, calcium ions regulate GlcAT-I expression through a signaling network comprising both suppressor (Cn-NFAT) and activator (TonEBP) molecules. In this way, by controlling both GAG and aggrecan synthesis, cells of the nucleus pulposus can autoregulate their own osmotic environment and accommodate mechanical loading.

Since cell function in the osmotically and mechanically stressed environment of the nucleus pulposus is dependent on the biosynthesis of aggrecan (2), we first evaluated the expression of GlcAT-I. This protein completes the synthesis of the common linker region of GAGs by transferring glucuronic acid to the core protein Gal-Gal-Xyl-*O*-Ser trisaccharide. Predictably, at both the mRNA and protein level, there was robust expression of GlcAT-I in nucleus pulposus cells of both the neonatal and mature rat discs; the protein was also expressed by cells of the annulus fibrosus. This latter observation was not unexpected, since the inner annulus, like the nucleus, is rich in proteoglycans (1, 2). Gain and loss of function experiments were performed to learn if calcium flux induced transcriptional activation of GlcAT-I reporter activity and if this activation was regulated by TonEBP. In the presence of ionomycin, suppression of TonEBP activity blocked induction of GlcAT-I; pTonEBP enhanced GlcAT-I reporter expression under basal conditions. Moreover, suppression of TonEBP in the absence of ionomycin also blocked GlcAT-I promoter activity, indicating that this transcription factor controlled basal gene expression. When GlcAT-I reporters that either lacked TonE site or contained a mutant TonE were treated with ionomycin, there was failure to increase activity. This observation lent strength to the findings reported above and indicated that TonEBP regulated GlcAT-I expression. We were able to confirm these findings using ChIP analysis and cells from TonEBP/NFAT5 null mice. ChIP analysis confirmed binding of TonEBP to TonE motif. Null MEFs displayed decreased basal GlcAT-I promoter activity and failure to induce reporter activity even when treated with ionomycin. Together, the results of these functional studies indicated that, in addition to regulating *tauT*, other osmolytes, and HSP-70 (4, 14, 21), by controlling the expression of GlcAT-I, TonEBP adapts nucleus pulposus cells to the mechanically and osmotically restrained conditions of the disc (4, 22).

The mechanism of activation of TonEBP is not completely understood, especially whether it is mediated by protein phosphorylation (23). In T cells and kidney cells, there is some evidence to indicate that regulation may be mediated by a phosphatase, Cn, which is activated by calcium ions (24, 25). The results of the studies described herein suggest that this mechanism may be cell type-specific. Treatment of nucleus pulposus cells with cyclosporine and FK506, agents that inhibit Cn signaling, failed to block induction of TonEBP or change the promoter activities of the TonEBP target gene *tauT*. Further support of the notion that Cn signaling was not required for TonEBP-dependent GlcAT-I promoter activation came from studies performed on TonEBP/NFAT5 null MEFs. We noted that, following ionomycin treatment, the null MEFs failed to induce GlcAT-I-D reporter activity, whereas both wild type and null cells did not induce activation of GlcAT-I-P construct. Although these results suggested that Cn signaling did not play a role in regulation of basal GlcAT-I expression, they did not elucidate role of Cn in the absence of TonEBP activity in nucleus pulposus cells.

To delineate the import of Cn in cells of the disc, we overexpressed catalytic (CnA) and regulatory (CnB) subunits and determined GlcAT-I reporter activity. Surprisingly, GlcAT-I promoter activity was suppressed; moreover, unlike wild type cells, ionomycin treatment of fibroblasts derived from Cn (CnA$\alpha$ and CnA$\beta$) null mice strongly induced GlcAT-I reporter activity. Of interest was the observation that, unlike in

nucleus pulposus cells and wild type NFAT5 MEFs, ionomycin treatment did not increase GlcAT-I-D reporter activity in Cn wild type fibroblasts, indicating cell type-specific differences. It is not unreasonable to assume that in these fibroblasts simultaneously with TonEBP, there is a strong induction of factors that negatively regulate the promoter activity, thereby neutralizing TonEBP-mediated induction.

Based on these studies, it is concluded that calcineurin signaling may be a negative regulator of GlcAT-I expression. The mechanism of suppression was not immediately obvious, since ionomycin simultaneously increased TonEBP-dependent GlcAT-I promoter activity. One possibility was that other members of the NFAT family may be involved in regulating GlcAT-I promoter activity. Relevant to this issue, it is well documented that Cn-mediated dephosphorylation of SP motifs results in the nuclear import of NFAT and stimulation of transcription (26). To address this issue, we overexpressed individual NFATs and determined GlcAT-I reporter activity. Since NFAT2, -3, and -4 but not NFAT1 decreased GlcAT-I promoter activity, it was concluded that GlcAT-I promoter activity was negatively regulated by these three NFATs but was independent of NFAT1. Activation of 3×NFAT luciferase reporter after co-transfection with NFAT expression plasmids confirmed that the expressed NFATs were functional in nucleus pulposus cells. Based on these findings and immunofluorescence experiments that document expression and activation of endogenous NFATs, we conclude that Cn-mediated activation of NFAT2, NFAT3, and NFAT4 serve an inhibitory role in governing GlcAT-I promoter activity in cells of the nucleus pulposus.

A recent study indicates that there are a number of Spl binding sites close to the transcription start site in the human GlcAT-I promoter (13). This study further showed that calcium promotes Spl activation through MEK/ERK signaling and subsequent binding to the motif between −65 and −56 bp influencing GlcAT-I expression (see Fig. 2) (13). Our studies confirmed that inhibition of Spl activity suppressed ionomycin-mediated induction of GlcAT-I promoter activity. Interestingly, ionomycin did not influence the activity of the GlcAT-I-P construct that lacked TonE but contained Spl motifs. Based on these findings, it is clear that Spl together with TonEBP regulates GlcAT-I promoter function. Moreover, specific to nucleus pulposus cells, our study shows that Spl activation alone is not sufficient for induction of GlcAT-I promoter activity, suggesting a cell type-specific regulation (13).

In summary, we demonstrate that calcium regulates expression of GlcAT-I, a critical enzyme required for GAG synthesis through TonEBP/NFAT5 and Cn-NFAT signaling pathways. Ongoing studies are being performed to test the hypothesis that changes in the activity of GlcAT-I are linked to the development of degenerative disc disease.

## REFERENCES


1. Feng, H., Danfelter, M., Strömqvist, B., and Heinegård, D. (2006) *J. Bone Joint Surg. Am.* **88,** 25–29
2. Setton, L. A., and Chen, J. (2006) *J. Bone Joint Surg. Am.* **88,** 52–57
3. Ng, L., Grodzinsky, A. J., Patwari, P., Sandy, J., Plaas, A., and Ortiz, C. (2003) *J. Struct. Biol.* **143,** 242–257
4. Tsai, T. T., Danielson, K. G., Guttapalli, A., Oguz, E., Albert, T. J., Shapiro, I. M., and Risbud, M. V. (2006) *J. Biol. Chem.* **281,** 25416–25424
5. Kitagawa, H., Ujikawa, M., and Sugahara, K. (1996) *J. Biol. Chem.* **271,** 6583–6585
6. Venkatesan, N., Barré, L., Benani, A., Netter, P., Magdalou, J., Fournel-Gigleux, S., and Ouzzine, M. (2004) *Proc. Natl. Acad. Sci. U. S. A.* **101,** 18087–18092
7. Bai, X., Wei, G., Sinha, A., and Esko, J. D. (1999) *J. Biol. Chem.* **274,** 13017–13024
8. Gouze, J. N., Bordji, K., Gulberti, S., Terlain, B., Netter, P., Magdalou, J., Fournel-Gigleux, S., and Ouzzine, M. (2001) *Arthritis Rheum.* **44,** 351–360
9. Alford, A. I., Yellowley, C. E., Jacobs, C. R., and Donahue, H. J. (2003) *J. Cell. Biochem.* **90,** 938–944
10. Parvizi, J., Parpura, V., Greenleaf, J. F., and Bolander, M. E. (2002) *J. Orthop. Res.* **20,** 51–57
11. Vijayagopal, P., and Subramaniam, P. (2001) *Atherosclerosis* **157,** 353–360
12. Fagnen, G., Phamantu, N. T., Bocquet, J., and Bonnamy, P. J. (1999) *J. Cell. Biochem.* **76,** 322–331
13. Barré, L., Venkatesan, N., Magdalou, J., Netter, P., Fournel-Gigleux, S., Ouzzine, M. (2006) *FASEB J.* **20,** 1692–1694
14. Ito, T., Fujio, Y., Hirata, M., Takatani, T., Matsuda, T., Muraoka, S., Takahashi, K., and Azuma, J. (2004) *Biochem. J.* **382,** 177–182
15. Lam, A. K., Ko, B. C., Tam, S., Morris, R., Yang, J. Y., Chung, S. K., and Chung, S. S. (2004) *J. Biol. Chem.* **279,** 48048–48054
16. Monticelli, S., and Rao, A. (2002) *Eur. J. Immunol.* **32,** 2971–2978
17. Ichida, M., and Finkel, T. (2001) *J. Biol. Chem.* **276,** 3524–3530
18. Clipstone, N. A., and Crabtree, G. R. (1992) *Nature* **357,** 695–697
19. Risbud, M. V., Guttapalli, A., Stokes, D. G., Hawkins, D., Danielson, K. G., Schaer, T. P., Albert, T. J., and Shapiro, I. M. (2006) *J. Cell. Biochem.* **98,** 152–159
20. Zeng, Y., Danielson, K. G., Albert, T. J., Shapiro, I. M., and Risbud, M. V. (2007) *J. Bone Miner. Res.* **22,** 1851–1861
21. Woo, S. K., Lee, S. D., Na, K. Y., Park, W. K., and Kwon, H. M. (2002) *Mol. Cell. Biol.* **22,** 5753–5760
22. Tsai, T. T., Guttapalli, A., Agrawal, A., Albert, T. J., Shapiro, I. M., and Risbud, M. V. (2007) *J. Bone Miner. Res.* **22,** 965–974
23. Jeon, U. S., Kim, J. A., Sheen, M. R., and Kwon, H. M. (2006) *Acta Physiol. (Oxf.)* **187,** 241–247
24. Trama, J., Lu, Q., Hawley, R. G., and Ho, S. N. (2000) *J. Immunol.* **165,** 4884–4894
25. Li, S. Z., McDill, B. W., Kovach, P. A., Ding, L., Go, W. Y., Ho, S. N., and Chen, F. (2007) *Am. J. Physiol.* **292,** C1606–C1616
26. Hogan, P. G., Chen, L., Nardone, J., and Rao, A. (2003) *Genes Dev.* **17,** 2205–2232

SPINE Volume 34, Number 14, pp 1448–1456


# Differential Phenotype of Intervertebral Disc Cells

## Microarray and Immunohistochemical Analysis of Canine Nucleus Pulposus and Anulus Fibrosus

Daisuke Sakai, MD, PhD,* Tomoko Nakai, BSc,* Joji Mochida, MD, PhD,* Mauro Alini, PhD,† and Sibylle Grad, PhD†

**Study Design.** Microarray gene expression profiling, quantitative gene expression analysis, and immunohistochemistry was used to investigate molecular variations between nucleus pulposus (NP) and anulus fibrosus (AF) of the dog intervertebral disc (IVD).

**Objective.** To identify specific molecules with differing expression patterns in NP and AF and compare their profile with articular cartilage (AC).

**Summary of Background Data.** Although experimental and animal studies have demonstrated the potential of cell based approaches for NP regeneration, there is still a deficiency of basic knowledge about the phenotype of IVD cells.

**Methods.** Comparative microarray analysis of beagle lumbar NP and AF was performed. Molecules of interest were evaluated by quantitative reverse transcriptase-polymerase chain reaction and immunohistochemistry, comparing lumbar and coccygeal NP and AF and AC. To assess interspecies variations, genes that had been found differentially expressed in rat tissues were also investigated.

**Results.** Forty-five genes with NP/AF signal log ratio ≥1 were identified. α-2-Macroglobulin, cytokeratin-18, and neural cell adhesion molecule (CD56) mRNA were higher in NP compared to AF and AC, and desmocollin-2 mRNA was higher in NP than AF. The expression profiles were similar in lumbar and coccygeal discs, although certain variations were noticed. Interspecies differences between rat and dog were evident in the expression of several genes. Immunohistochemistry confirmed differences in gene expression at the protein level.

**Conclusion.** This study reports on the expression of molecules that have not been described previously in IVD, in non-notochordal discs comparable with human. Interspecies differences were noted between rat and dog tissues, whereas variations between caudal and lumbar discs were less prominent. The NP of the beagle as a chondrodystrophoid dog breed is potentially more similar to the human than the NP of species whose discs do not naturally degenerate. Therefore, studies on appropriate species may contribute to a better understanding of the cell types residing in the IVD.

From the *Department of Orthopaedic Surgery, Surgical Science, Tokai University School of Medicine, Isehara, Kanagawa, Japan; and †Biomaterials and Tissue Engineering Program, AO Research Institute, Davos, Switzerland.

Acknowledgment date: August 5, 2008. First revision date: October 8, 2008. Acceptance date: January 19, 2009.

The manuscript submitted does not contain information about medical device(s)/drug(s).

No funds were received in support of this work. No benefits in any form have been or will be received from a commercial party related directly or indirectly to the subject of this manuscript.

Address correspondence and reprint requests to Sibylle Grad, PhD, AO Research Institute, Clavadelerstrasse 8, CH 7270 Davos, Switzerland; E-mail: sibylle.grad@aofoundation.org

**Key words:** Microarray, gene expression, immunolocalization, nucleus pulposus, anulus fibrosus, canine, chondrodystrophoid. **Spine 2009;34:1448–1456**

Intervertebral disc (IVD) degeneration, although in many cases asymptomatic, is associated with low back pain and diseases such as sciatica, disc herniation, or prolapse.[1,2] It implies a decrease in disc height and alterations in the mechanics of the spinal column, and in the long term it can lead to spinal stenosis, a major cause of pain and disability, especially in the elderly. The incidence of IVD degeneration is increasing exponentially, and it is increasingly recognized as a disorder that also affects the younger population. In fact, about 20% of people in their teens have discs with mild signs of degeneration.[3,4]

In view of the fact that current treatment methods may reduce pain but cannot repair the degenerated disc, there is an increasing interest in novel cell-based therapies. Their aim is to achieve cellular repair of the degenerated disc matrix to ultimately restore disc height and biomechanical function. One approach has been to stimulate the disc cells to increase the rate of matrix synthesis by application of growth factors or gene therapy.[5–8] However, because cell densities in human discs are low and their vitality in degenerate discs is impaired, stimulation of the remaining cells may be insufficient.[9] Cell implantation may overcome the paucity of cells in a degenerate disc. For cell therapy, mesenchymal stem cells have been proposed, and clinical procedures have been developed to inject these cells into a degenerated disc.[10–12] It has also been suggested that, similar to chondrogenic differentiation, mesenchymal stem cells can differentiate toward the NP cell phenotype *in vitro*.[13–15]

Although experimental work and animal studies have demonstrated the potential of cell-based approaches, there is still a deficiency of basic knowledge about the cellular components residing in the IVD. In a healthy disc, the cells of the nucleus pulposus (NP) function to maintain its highly hydrated gelatinous matrix, which is rich in proteoglycans and in collagen and elastin fibers. The NP is surrounded by the anulus fibrosus (AF), which is composed of a series of concentric lamellae, consisting of collagen and elastin fibers. Whereas the cells of the outer AF appear fibroblast-like and elongated, the NP cells in human adults are described as chondrocyte-like because of their

rounded morphology and their phenotypic profile. The NP and AF cells are generally referred to as IVD cells or chondrocytes, although they markedly differ from each other and from articular cartilage cells. Appropriate molecular markers that define NP and AF cells and differ from chondrocyte markers would be instrumental in evaluating and monitoring a cell population with respect to the IVD-like phenotype.

In a previous study, we reported a number of genes that were differentially expressed in NP, AF, and AC cells in rats.[16] Although distinct animal models are useful to investigate specific associations, considerable variations between species are evident, and findings cannot be translated from one to another species without careful consideration.[17] The present study used discs from dog of a chondrodystrophoid breed and microarray, quantitative reverse transcriptase-polymerase chain reaction (RT-PCR) and immunohistochemistry to identify potential new molecules with varying expression in NP and AF. Furthermore, because caudal discs are often used as models to study IVD biology and biomechanics, potential differences between caudal and lumbar discs were assessed with respect to the molecules of interest. Finally, the expression of the genes that had been found differentially expressed in the rat was also analyzed in the dog tissues. This allowed evaluating interspecies differences and similarities between animals with notochordal *versus* chondrocytic nucleus, which is of fundamental importance for the selection of a particular animal model to study IVD degeneration and regeneration.[17]

## ■ Materials and Methods

### *Microarray Analysis*

All animal experiments were carried out according to the protocol approved by the Animal Experimentation committee at our institution (experiment #042015). Mature female beagle dogs (16–18 months old; n = 3; mean weight approximately 10 kg; Nosan Beagle, Nosan Corp., Kanagawa, Japan) were used for tissue harvest for microarray analysis. NP and AF were harvested from lumbar (L2–L3 to L5–L6) and caudal (C1/2 to C4/5) discs in an aseptic environment. Tissue samples were immediately placed in RNA*later* (Ambion, Austin, TX) and sent for microarray analysis service to Kurabo Industries Inc., Biomedical Dept., Osaka, Japan. This service included high-quality total RNA isolation, cDNA synthesis, biotin-labeled cRNA synthesis, cohybridization (NP/AF) to the Affymetrix GeneChip Dog Genome Array (Affymetrix Inc., Santa Clara, CA), array imaging, and analysis according to the protocol provided by the manufacturer (Affymetrix GeneChip Expression Analysis Technical Manual).[18,19] A total of 3 microarrays were prepared: NP/AF cohybridizations, each with dye-swap to exclude dye bias. The relative expression of each gene in NP *versus* AF was expressed as a ratio of fluorescence intensities.

### *Real-time RT-PCR*

NP and AF were dissected from the lumbar (n = 9) and coccygeal (n = 4) discs as specified above. Articular cartilage was harvested from femoral condyles (n = 9) of the same animals. Chopped tissue samples were placed in Isogen (Nippon Gene, Toyama, Japan), frozen in liquid nitrogen, and homogenized with a Polytron homogenizer. Total RNA was extracted by a modified TRISpin method,[20] using the SV Total RNA Isolation System (Promega, Madison, WI). Reverse transcription was performed with TaqMan reverse transcription reagents (Applied Biosystems, Foster City, CA) and random hexamer primers.

For real-time PCR, 5 genes were selected that showed a high signal ratio in the NP *versus* AF microarray comparison: α-2-macroglobulin (A2M), annexin A4 (ANXA4), desmocollin 2 (DSC2), cytokeratin 18 (CK18), and neural cell adhesion molecule 1 (NCAM1, CD56 140-kDa isoform). In addition, 5 genes, that had been found differently expressed in NP *versus* AC in the rat, were evaluated[16]: Cartilage oligomeric matrix protein (COMP), glypican 3 (GPC3), matrix Gla protein (MGP), pleiotrophin (PTN), and vimentin (VIM). Dog primers (Invitrogen, Carlsbad, CA) and TaqMan probes (Sigma, St. Louis, MO) were designed using Primer Express software, version 3.0 (Applied Biosystems) (Table 1). The assay for amplification of 18S ribosomal RNA was from Applied Biosystems. PCR was performed on a 7300 Real-Time PCR System (Applied Biosystems) with TaqMan Universal PCR Master Mix (Applied Biosystems), 900 nmol/L primers (forward and reverse), and 250 nmol/L TaqMan probe. Relative quantification of target mRNA was performed according to the comparative $C_T$ method (ABI PRISM User Bulletin 2, Applied Biosystems) with 18S ribosomal RNA as the endogenous control. Gene expression levels of lumbar and coccygeal NP and AF were normalized to the values of their corresponding AC.

Statistical significance was determined with SPSS 14.0 software, using Kruskal-Wallis nonparametric analysis with Mann-Whitney *U post hoc* testing, and $P < 0.05$ was defined as significant.

### *Immunohistochemistry*

Mouse anti-CD56 (NCAM1) (Clone 123C3) was purchased from Spring Bioscience (Montigny le Bretonneux, FR) and applied in the dilution 1:50; Rabbit anti-alpha 2 macroglobulin from GeneTex, Inc. (San Antonio, TX) was applied in the dilution 1:50; Rabbit anti-desmocollin 2 from Progen Biotechnik (Heidelberg, Germany) was applied in the dilution 1:50; Rabbit anti-glypican 3 (aa 303–464) from Santa Cruz Biotechnology (Santa Cruz, CA) was applied in the dilution 1:25; Mouse anti-cytokeratin 18 (Clone C-04) from Novus Biologicals, Inc. (Littleton, CO) was applied in the dilution 1:50.

Lumbar IVD, coccygeal IVD, and AC from the femoral condyle were harvested from 12-month-old female beagle dogs and fixed in 4% paraformaldehyde. Tissues were decalcified, embedded in paraffin, and cut into 3–5 μm sagittal sections. Sections were incubated with 0.005% proteinase (Sigma) at 37°C for 10 minutes and probed with relevant primary antibodies at 4°C for 16 hours. Subsequently, they were treated with appropriate biotinylated secondary antibodies at room temperature for 1 hour. Slides were then processed using Vectastain ABC Kit (Vector Laboratories), developed with 3,3'-diaminobenzidine (DAB) substrate and counterstained with hematoxylin.

For detection of CK18, tissues were embedded in OCT compound and cryosectioned into 6-μm-thick sections. IVD tissues were not decalcified and sectioned axially. Cryosections were incubated with primary antibody at 4°C for 16

**Table 1. Oligonucleotide Primers and Probes Used for Real-Time PCR**

| Gene Name | Gene Symbol | Ref. Sequence | Primer Fw (5'-3') | Primer Rev (5'-3') | Probe (5'-FAM; 3'-TAMRA) |
|---|---|---|---|---|---|
| α-2-Macroglobulin | A2M | XM_534893 | ACT TGG CTC ACT GCC TTT GTA CT | GTT GAG CAG AGA CCC GGA ACT | AGC ACA CAT CAC CCA AGC CCT CAT G |
| Annexin A4 | ANXA4 | NM_001003039 | CCC AGC GCC AGG AGA TTA G | CGA CTT CAG GTC GTC CAT CA | ACG GCC TAC AAG AGC ACC ATC GGC |
| Cartilage oligomeric matrix protein | COMP | XM_533869 | GCC GAG ACA CGG ATT TGG | CAC GTC CTC TTG CCC TGA GT | TTC CCC GAC GAG AAG CTC CGC |
| Desmocollin 2 | DSC2 | XM_537291 | ACG ATG CAC ACA CGT CTC AAA | TGG TGA TCA CGC CTG TAG TTG | CCA TCA TCG AGC AGT TGC CAG CGT A |
| Glypican 3 | GPC3 | XM_538178 | CAG CCT CTT TCC AGT CAT CTA CAC | CCC CTC GGA GGC ACT CAT | AGC TCA TGA ACC CCG GCC TGC |
| Cytokeratin 18 | CK18 | XM_849849 | AAG AAC CAC GAG GAG GAA GTA AAG | CCC GGA TAT CTG CCA TGA TC | TCT ACA AAA CCA AAT CGC CAA CTC TGG G |
| Matrix Gla protein | MGP | XM_848662 | CCA CCA AGC CCG CCT AT | GCG TAG CGT TCG CAA AGC | CTC AAC CGG GAA GCC TGT GAT GAC TTC |
| Neural cell adhesion molecule 1 (CD56 140-kDa isoform) | NCAM1 | NM_001010950 | AAG ACT CTG GAC GGG CAC AT | GGC GTC TGT GTA CTG GAT GCT | TGC GTA GCC ATG CCC GCG |
| Pleiotrophin | PTN | XM_532732 | GTG CAG CAG CGT CGA AAA | TGT CCA CAG CTG CCA AGA TG | TGC AGC TGC CTT CCT GGC ATT CAT |
| Vimentin | VIM | XM_844468 | CAG GCG AAG CAG GAG TCA AC | TCC CTT TGA GTG CAT CCA CTT | CCG GAG CCA GGT GCA GTC CCT C |

Probes were labeled with the reporter dye molecule FAM (6-carboxyfluorescein) at the 5' end and with the quencher dye TAMRA (6-carboxy-N, N, N', N'-tetramethylrhodamine) at the 3' end.

hours. Subsequently, sections were treated with anti-mouse Alexa Fluor 488 goat secondary antibody (1:200, Molecular Probes, Invitrogen). Nuclei were counterstained with 4',6-diamidino-2-phenylindole (DAPI) and slides observed with fluorescence microscopy.

## ■ Results

### *Microarray*

A comparative microarray analysis using the Affymetrix GeneChip Dog Genome Array, which are high-density oligonucleotide arrays (11-μm spots) containing 2,383,625-mer probe-sets detecting 21,700 transcripts was performed to identify genes that may be used to uniquely distinguish NP from AF cells. As we were particularly interested in potential NP marker molecules, the focus was laid on molecules with a high NP *versus* AF expression ratio. While examining the signal ratios in the NP *versus* AF microarray comparison, 45 genes with a signal log ratio of at least 1 were noted (Table 2). Furthermore, 77 genes had a signal log ratio of −1 or lower, 43 of which showed a ratio of −3 or lower (Table 3).

Eight genes were identified with an NP to AF signal log ratio higher than 3: Wnt inhibitory factor-1, CK18, A2M, desmoplakin, DSC2, UDP-glucose dehydrogenase, carbonic anhydrase II, and ADAMTS10. Among these genes, CK18, A2M, and DSC2 were selected for quantitative analysis by real-time RT-PCR, as they appeared valuable candidate genes for the characterization of NP cells. In addition, 2 genes with a signal log ratio of 1.4, namely, ANXA4 and NCAM1 (CD56), were further investigated.

### *Real-Time PCR*

Data from lumbar discs are illustrated in Figure 1. In correlation with the microarray results, A2M, DSC2, CK18, and NCAM1 (CD56) mRNA levels were higher in NP compared to AF. The NP gene expression of A2M, CK18, and NCAM1 (CD56) was also enhanced when compared to AC, whereas no difference was noted in DSC2 gene expression between NP and AC. No differences in ANXA4 mRNA expression levels were found between NP, AF, and AC.

In contrast to previous findings in the rat, the GPC3 mRNA expression was equally low in NP as in AC. Hence, GPC3 expression was downregulated in the dog compared to the rat NP, while its expression was higher in dog AF than AC, which is similar to the rat results. The COMP, MGP, and VIM expression levels were lower in NP than in AF and AC, whereas PTN was lower in NP compared to AC. Additionally, MGP, PTN, and VIM mRNA values were lower in AF compared to AC.

Results from the coccygeal discs are illustrated in Figure 2, with data from the corresponding lumbar NP and AF shown for comparison. Essentially, the expression profile of the genes analyzed was similar in lumbar and coccygeal discs, showing stronger expression of A2M, CK18, and NCAM1 (CD56) in NP compared with AF and AC and higher DSC2 expression in NP than AF. In addition, GPC3 expression was significantly higher in coccygeal AF than NP. The mRNA expression of COMP, MGP, and PTN also demonstrated a similar pattern in coccygeal as in lumbar disc, showing lower expression levels in NP as compared to AC and higher AF than NP levels of COMP mRNA.

Variations between coccygeal and lumbar disc were noticed for NCAM1 (CD56), which was expressed more highly in coccygeal than in lumbar NP, and for PTN and VIM, which were expressed more highly in

**Table 2. Genes With a Signal Log Ratio of 1 or Higher in the NP *Versus* AF Microarray Comparison**

| Signal Log Ratio | Signal Log Ratio Low | Signal Log Ratio High | Change in *P* | Representative Public ID | Gene Title | Gene Symbol |
|---|---|---|---|---|---|---|
| 5.2 | 4.9 | 5.5 | 0.00002 | CO629970 | Similar to WIF-1 | LOC481148 |
| 4.5 | 3.3 | 5.8 | 0.00006 | CO673880 | Similar to Keratin, type I cytoskeletal 18 (Cytokeratin 18) (K18) (CK 18) | LOC477601 |
| 3.7 | 3.3 | 4 | 0.00002 | CO664742 | Similar to alpha 2 macroglobulin | LOC477699 |
| 3.5 | 2.8 | 4.1 | 0.00002 | CO704199 | Similar to Desmoplakin (250/210 kDa paraneoplastic pemphigus antigen) | LOC488207 |
| 3.4 | 2.2 | 4.6 | 0.000023 | CO614128 | Desmocollin type 2 | DSC2 |
| 3.4 | 1.5 | 5.2 | 0.000618 | CO678462 | Similar to UDP-glucose dehydrogenase | LOC479106 |
| 3.3 | 3 | 3.5 | 0.00002 | CF409351 | Similar to carbonic anhydrase II (carbonate dehydratase II) (CA-II) (carbonic anhydrase C) | LOC477928 |
| 3.2 | 1.3 | 5.1 | 0.000492 | CF409176 | Similar to ADAMTS-10 (A disintegrin and metalloproteinase with thrombospondin motifs 10) (ADAM-TS 10) | LOC478077 |
| 3 | 0.9 | 5.2 | 0.000692 | AB049597.1 | Epidermal growth factor | CEGF |
| 2.7 | 2.2 | 3.3 | 0.00002 | CO593864 | Somatostatin receptor 2 | SSTR2 |
| 2.4 | 0.4 | 4.3 | 0.000189 | U16208.1 | Fibronectin 1 | FN1 |
| 2 | 1.6 | 2.4 | 0.00002 | AB085580.1 | Caspase-3 | CASP3 |
| 2 | 1.9 | 2.1 | 0.00002 | CO585869 | Dystonin | DST |
| 1.9 | 1 | 2.8 | 0.00013 | AF133250.1 | Vascular endothelial growth factor 188 | VEGF |
| 1.9 | 1.6 | 2.1 | 0.00002 | CO697517 | Similar to fibrinogen-like protein 1 precursor (Hepatocyte-derived fibrinogen-related protein 1) (HFREP-1) (Hepassocin) (HP-041) | LOC475617 |
| 1.9 | 0.6 | 3.2 | 0.000023 | CO619157 | Similar to basic beta 1 syntrophin | LOC482030 |
| 1.8 | 1 | 2.5 | 0.000027 | AY305401.1 | Somatostatin receptor 2 | SSTR2 |
| 1.8 | 1.7 | 2 | 0.00002 | CF411593 | Similar to UDP-Gal:betaGlcNAc beta 1,4- galactosyltransferase 4 | LOC487991 |
| 1.8 | 1.3 | 2.3 | 0.00002 | CO698628 | Similar to 78-kDa glucose-regulated protein precursor (GRP 78) (Immunoglobulin heavy chain-binding protein) (BiP) | LOC480726 |
| 1.7 | 1 | 2.5 | 0.000023 | CO601750 | Similar to DnaJ (Hsp40) homolog, subfamily C, member 3 | LOC476966 |
| 1.7 | 0.5 | 3 | 0.000241 | CO696669 | Similar to notch1 preproprotein | LOC480676 |
| 1.6 | 1.1 | 2 | 0.000167 | BM537581 | Translocation-associated membrane protein 1 | TRAM1 |
| 1.6 | 0.9 | 2.2 | 0.000068 | CO710930 | Mucin | LOC404014 |
| 1.6 | 1.4 | 1.7 | 0.00002 | CO703865 | Similar to cyclin G1 (Cyclin G) | LOC479303 |
| 1.6 | 1.3 | 1.8 | 0.00002 | AJ407826 | Similar to heat shock cognate 71 kDa protein | LOC479406 |
| 1.5 | 1.2 | 1.8 | 0.00002 | CO715646 | Similar to heat shock protein 1, beta | LOC474919 |
| 1.4 | 0.3 | 2.4 | 0.000692 | BU744786 | CD56 140 kDa isoform | LOC479435 |
| 1.4 | 1.2 | 1.7 | 0.00002 | D38223.1 | Annexin A4 | ANXA4 |
| 1.4 | 1.1 | 1.7 | 0.00003 | AF201729.1 | Matrix metalloproteinase-13 | MMP13 |
| 1.4 | 1.1 | 1.8 | 0.00002 | BU751122 | Similar to junctional adhesion molecule 3 precursor | LOC489271 |
| 1.4 | 1 | 1.8 | 0.000273 | CO666324 | Similar to cyclin G2 | LOC478442 |
| 1.3 | 0.9 | 1.8 | 0.000241 | CO635035 | Estrogen-regulated LIV-1 protein | LIV-1 |
| 1.3 | 1 | 1.5 | 0.001336 | AF084483.1 | Muscarinic acetylcholine receptor m2 | CHRM2 |
| 1.3 | 0.8 | 1.7 | 0.00002 | CO584391 | Similar to osteopontin precursor (bone sialoprotein 1) (Secreted phosphoprotein 1) (urinary stone protein) (nephropontin) (uropontin) | LOC478471 |
| 1.2 | 1.1 | 1.2 | 0.00002 | DG8-215h9-939b11.r1ca | Fibronectin 1 | FN1 |
| 1.2 | 0.9 | 1.4 | 0.00002 | U52106.1 | Fibronectin 1 | FN1 |
| 1.1 | 0.6 | 1.6 | 0.000023 | U52105.1 | Fibronectin 1 | FN1 |
| 1.1 | 0.5 | 1.6 | 0.001201 | CO672418 | Dystonin | DST |
| 1.1 | 1 | 1.2 | 0.00002 | CO675662 | Metallothionein-1 | LOC403800 |
| 1.1 | 0.3 | 1.9 | 0.000101 | DG2-97k24-149d4.r1ca | Similar to pleiotrophin precursor–mouse similar to pleiotrophin precursor–mouse | LOC475509/LOC480079 |
| 1 | 0.8 | 1.1 | 0.00002 | AF211257.1 | Fibroblast growth factor receptor 2 | FGFR2 |
| 1 | 0.8 | 1.2 | 0.00002 | AF525493.1 | Heat shock 27-kDa protein 8 | HSPB8 |
| 1 | 0.5 | 1.4 | 0.000027 | AF060562.1 | Basic fibroblast growth factor | BFGF |
| 1 | 0.8 | 1.2 | 0.00002 | CO603430 | Dystonin | DST |
| 1 | 0.4 | 1.5 | 0.000492 | CO693021 | Similar to chloride intracellular channel protein 4 (mc3s5/mtCLIC) | LOC487367 |
| 1 | 0.8 | 1.1 | 0.000078 | BM538976 | Similar to 60-kDa heat shock protein, mitochondrial precursor (60 kDa chaperonin) (heat shock protein 60) (mitochondrial matrix protein P1) (P60 lymphocyte protein) | LOC478854 |
| 1 | 0.7 | 1.3 | 0.00002 | CO625323 | Similar to bone morphogenetic protein 6 | LOC478715 |
| 1 | -0.1 | 2.1 | 0.00003 | CF407676 | Similar to crystallin, ζ-like 1 isoform a | LOC478408 |

Shaded boxes indicate genes analyzed by RT-PCR.

**Table 3. Genes With Signal Log Ratio of (−3) or Lower in the NP *Versus* AF Microarray Comparison**

| Signal Log Ratio | Signal Log Ratio Low | Signal Log Ratio High | Change in *P* | Representative Public ID | Gene Title | Gene Symbol |
|---|---|---|---|---|---|---|
| −8.9 | −12.4 | −5.4 | 0.99998 | CO702793 | Phosphoenolpyruvate carboxykinase | PEPCK |
| −7.3 | −10 | −4.6 | 0.99997 | CO585446 | Similar to Laminin β-1 chain precursor (Laminin B1 chain) | LOC475883 |
| −7.2 | −9.1 | −5.2 | 0.99998 | AF099154.1 | Von Willebrand factor | VWF |
| −7.2 | −9.2 | −5.1 | 0.99998 | CO698338 | MHC class II DR alpha chain | DLA-DRA1 |
| −6.9 | −8.5 | −5.3 | 0.99998 | M29611.1 | MHC class II DLA DRB1 beta chain | DLA-DRB1 |
| −6.2 | −7.2 | −5.3 | 0.99998 | AF153062.1 | Type I collagen pre-pro-alpha1(I) chain | COL1A1 |
| −6.1 | −9.6 | −2.6 | 0.999562 | CO613060 | Similar to collagen type XIV | LOC475085 |
| −6 | −6.2 | −5.8 | 0.99998 | DG14-68n1-973g20.r1ca | Type I procollagen pro-alpha 2 chain | COL1A2 |
| −5.7 | −7.9 | −3.5 | 0.99998 | BU746128 | Cathepsin S | CTSS |
| −5.7 | −7.8 | −3.6 | 0.99998 | DG14-67c3-973h12.r1ca | Similar to β-tropomyosin | LOC481598 |
| −5.4 | −7.5 | −3.4 | 0.99998 | AB011373.1 | Aquaporin 1 | AQP1 |
| −5.4 | −7.7 | −3.1 | 0.999965 | CO702048 | Similar to CD163 antigen isoform a | LOC477704 |
| −5.2 | −7 | −3.4 | 0.99998 | U66246.1 | Von Willebrand factor | VWF |
| −5.2 | −5.8 | −4.7 | 0.99998 | CO709518 | Similar to myosin light chain 3 | LOC478896 |
| −5.2 | −8.1 | −2.4 | 0.999977 | CO718911 | Similar to caveolin 3 | LOC484671 |
| −5.1 | −5.4 | −4.7 | 0.99998 | CO709482 | Myosin, light polypeptide 2, regulatory, cardiac, slow | MYL2 |
| −5.1 | −5.5 | −4.6 | 0.99998 | BU745565 | Slow myosin heavy chain | MYH7 |
| −5.1 | −6.3 | −3.9 | 0.99998 | CO719197 | Similar to myoglobin | LOC481283 |
| −5.1 | −5.6 | −4.6 | 0.99998 | BU745233 | Similar to troponin C, slow | LOC476595 |
| −5 | −6.9 | −3.1 | 0.999977 | CO711833 | Similar to Chloride intracellular channel 2 | LOC492270 |
| −4.9 | −5.3 | −4.4 | 0.99998 | CO657313 | Similar to hemoglobin beta chain-dog | LOC480784 |
| −4.8 | −6.9 | −2.7 | 0.999562 | CO666771 | Similar to integrin α-7 precursor (UNQ406/PRO768) | LOC481097 |
| −4.8 | −7.3 | −2.2 | 0.999954 | CO598893 | Similar to integrin β4 precursor (GP150) (CD104 antigen) | LOC483318 |
| −4.6 | −6.8 | −2.4 | 0.999911 | BU749834 | Cardiac titin | TTN |
| −4.6 | −5.3 | −3.9 | 0.999932 | CF412378 | Myosin, light polypeptide 2, regulatory, cardiac, slow | MYL2 |
| −4.5 | −5.4 | −3.7 | 0.99997 | AF111100.1 | Matrix metalloproteinase-2 | MMP-2 |
| −4.5 | −6.1 | −3 | 0.99998 | BU744374 | Triadin | TRDN |
| −4.5 | −7.2 | −1.7 | 0.99996 | CO608832 | Similar to collagen type XIV | LOC475085 |
| −4.4 | −6 | −2.9 | 0.99751 | CO713963 | Similar to neuropilin-1 precursor (Vascular endothelial cell growth factor 165 receptor) | LOC477955 |
| −4.2 | −6.5 | −1.9 | 0.999977 | AY156692.1 | Cathepsin S | CTSS |
| −4.2 | −6.4 | −1.9 | 0.999693 | DG9-119a21-441b5.r1ca | Similar to adenylate cyclase 2 | LOC480271 |
| −4.2 | −5.2 | −3.2 | 0.99998 | CO586808 | Similar to fibulin 2, precursor | LOC484634 |
| −4 | −5.6 | −2.5 | 0.999922 | CO674494 | Cathepsin S | CTSS |
| −3.6 | −5.1 | −2.2 | 0.999781 | CO701916 | Similar to enolase 3, beta | LOC479469 |
| −3.5 | −4.6 | −2.5 | 0.999308 | BU748808 | Similar to filamin | LOC481084 |
| −3.3 | −5.1 | −1.6 | 0.999965 | U32086.1 | Vascular cell adhesion molecule-1 | VCAM1 |
| −3.3 | −5.3 | −1.3 | 0.99998 | BM539480 | β-actin, similar to cytoplasmic β-actin | ACTB/LOC479083 |
| −3.3 | −4.2 | −2.3 | 0.99996 | AY134865.1 | Cardiac titin | TTN |
| −3.3 | −5.4 | −1.2 | 0.999954 | L08254.1 | Phenylalanine hydroxylase | PAH |
| −3.2 | −3.6 | −2.9 | 0.99998 | DG2-59i4-199b11.r1ca | Similar to alpha 1 type XII collagen long isoform precursor | LOC481881 |
| −3 | −4.8 | −1.1 | 0.999922 | L31625.1 | Intercellular adhesion molecule-1 | ICAM-1 |
| −3 | −3.5 | −2.4 | 0.999977 | BU744706 | Collagen type IV alpha 2 chain | COL4A2 |
| −3 | −4.3 | −1.7 | 0.999973 | DG14-126l3-1074k14.r1ca | Uncoupling protein 3 | UCP3 |

coccygeal than in lumbar AF. Comparing results obtained from dog with rat tissues, the relative *COMP* and *MGP* gene expression was similar in the dog and the rat, whereas interspecies differences were evident in the expression of *GPC3*, *PTN*, and *VIM*.

### *Immunohistochemistry*

Basically, observations with respect to differences in gene expression were confirmed at the protein level. A strong immunopositive signal for A2M was observed in the coccygeal NP. The staining was cell-associated and mainly intracellular. Although some A2M-negative cells were seen, the majority of the NP cell clusters reacted positive for A2M. In lumbar NP, the A2M immunoreaction appeared weaker than in the coccygeal NP. Nevertheless, most lumbar NP cells also showed positive staining. However, A2M immunoreactivity was not observed in lumbar and coccygeal AF and in AC (Figure 3).

Comparing DSC2 staining in NP, AF, and AC, most immunopositive cells were noted among articular chondrocytes. Staining was cell-associated and was evident in the middle and deep zones of the cartilage. Both lumbar and coccygeal NP also had DSC2 positive cells, whereas AF tissues were immunonegative (Figure 4).

Positive staining for NCAM1 (CD56) was noticed in a small proportion of colonized lumbar NP cells. Higher numbers of colonized NP cells that reacted positively were seen in the coccygeal discs. Both AF and AC were negative for NCAM1 (CD56) (Figure 5).

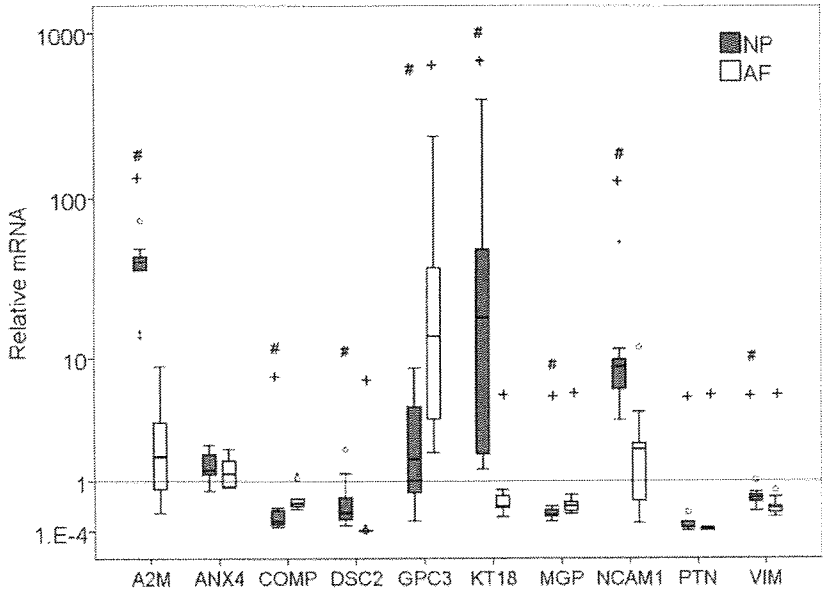


Figure 1. Relative mRNA expression of nucleus pulposus (NP) and anulus fibrosus (AF) tissue isolated from intervertebral discs of beagle dog lumbar spine. Data are expressed relative to the levels of articular cartilage (AC). $+P < 0.05$ *vs.* AC; $\#P < 0.05$ *vs.* AF; n = 9.

The expression of CK18 was visualized by immunofluorescence. A strong signal was associated with the majority of both lumbar and coccygeal NP cells. Articular chondrocytes also showed a positive reaction, although numerous cells in AC were CK18 negative. Similar results were obtained for AF cells. Generally, the CK18 staining was weaker in AF than in NP sections (Figure 6).

Immunoreactivity for GPC3 was observed only in the coccygeal AF, where the staining was localized intracellularly (Figure 7). GPC3 was not detectable in lumbar AF, NP, and AC tissues (not shown).

## ■ Discussion

With the aim to elucidate differences between different cell types present in the IVD, previous studies have addressed phenotypic characteristics and matrix production.[21,22] Whereas those investigations primarily focused on the expression and synthesis of matrix molecules such as collagens and proteoglycans, this extended study used large-scale gene expression profiling to identify differences in the expression patterns of NP and AF cells. Cartilage was included into RT-PCR and immunohistochemical examination because of the close similarities between IVD cells and articular chondrocytes.[21,22] We have previously reported on a related study using rat cells and tissues.[16] In the present study, we opted for the beagle dog because this breed is known as chondrodystrophoid, which – in contrast to the rat – lacks a notable notochordal cell population in the NP after birth and is therefore more similar to that found in humans.[23,24]

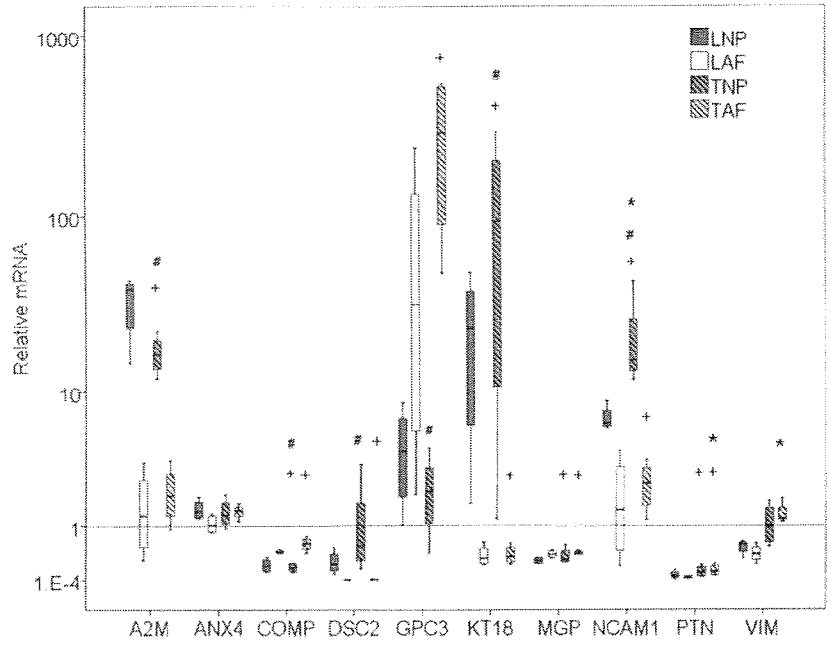


Figure 2. Relative mRNA expression of nucleus pulposus (TNP) and anulus fibrosus (TAF) tissue isolated from intervertebral discs of beagle dog tail. Expression of the corresponding lumbar disc nucleus pulposus (LNP) and anulus fibrosus (LAF) is shown for comparison. Data are expressed relative to the levels of articular cartilage (AC). $+P < 0.05$ *vs.* AC; $\#P < 0.05$ *vs.* TAF; $*P < 0.05$ *vs.* lumbar; n = 4.

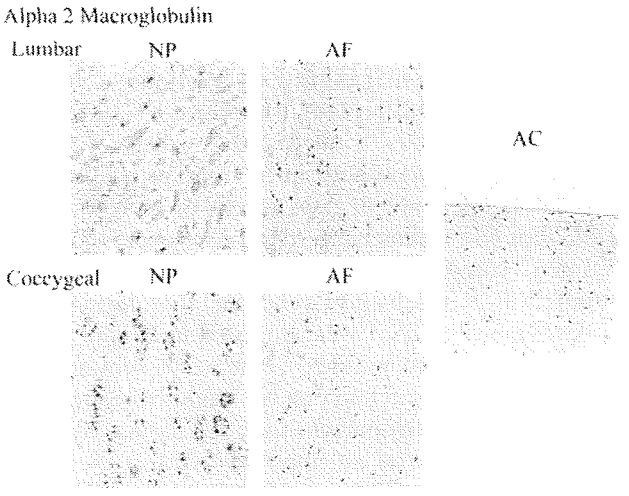


Figure 3. Immunolocalization of $\alpha$-2-macroglobulin in lumbar and coccygeal nucleus pulposus (NP). The majority of NP cells stain positive, whereas lumbar and coccygeal anulus fibrosus (AF) and articular cartilage (AC) cells are immunonegative. Scale bars: 200 $\mu$m.

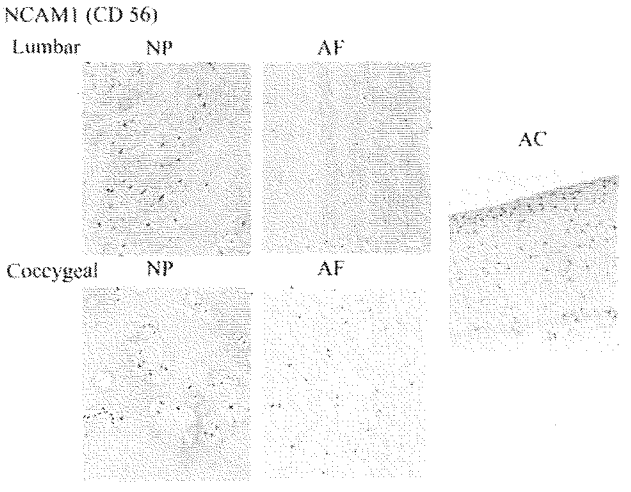


Figure 5. Immunolocalization of neural cell adhesion molecule 1 (CD56) in lumbar and coccygeal nucleus pulposus (NP). The majority of coccygeal and a smaller proportion of lumbar NP cells stain positive, whereas lumbar and coccygeal anulus fibrosus (AF) and articular cartilage (AC) cells are immunonegative. Scale bars: 200 $\mu$m.

In this microarray analysis of mature female beagle dogs, 45 genes were found with a high ($\geq$1) NP/AF signal log ratio, whereas 77 genes had a low ($\leq -1$) NP/AF ratio. Even though these data originate from 3 independent microarray analyses, they can be considered neither as comprehensive nor conclusive. The aim was to identify potential candidate genes that were further investigated by quantitative RT-PCR. The selection for RT-PCR was primarily focused on genes with a high NP/AF signal ratio in the microarray. Generally, results from the microarray analysis were confirmed at gene expression and for the most part also at protein levels. However, although ANXA4 was expressed significantly more highly in NP compared to AF in the microarray analysis, this difference could not be confirmed by real-time RT-PCR. It is important to consider that with the capability to screen large proportions of a genome, microarrays have the disadvantages of a certain lack in both sensitivity and specificity, which is associated with a considerable proportion of false positives.[25,26] Possible reasons for the disagreement between microarray and quantitative RT-PCR may include recognition of alternative transcripts, cross-hybridization, and signal quantification techniques, among others. Furthermore, different animals, although of the same age and sex, were used for microarray and RT-PCR analysis, which may also account for the observed divergences. Taken together, this

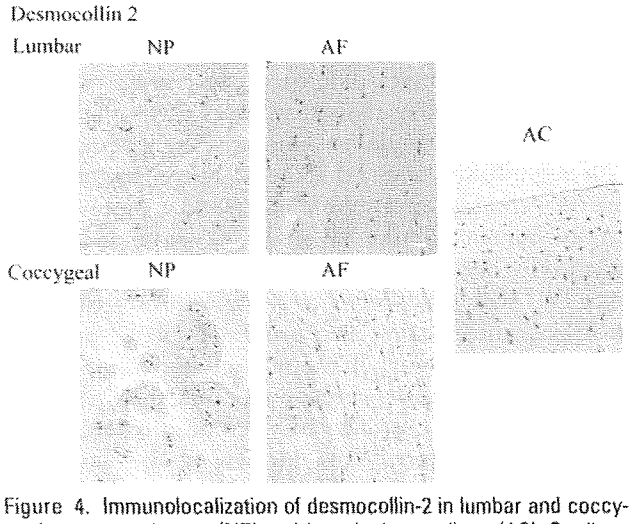


Figure 4. Immunolocalization of desmocollin-2 in lumbar and coccygeal nucleus pulposus (NP) and in articular cartilage (AC). Cartilage and a proportion of NP cells stain positive, whereas anulus fibrosus (AF) cells are immunonegative. Scale bars: 200 $\mu$m.

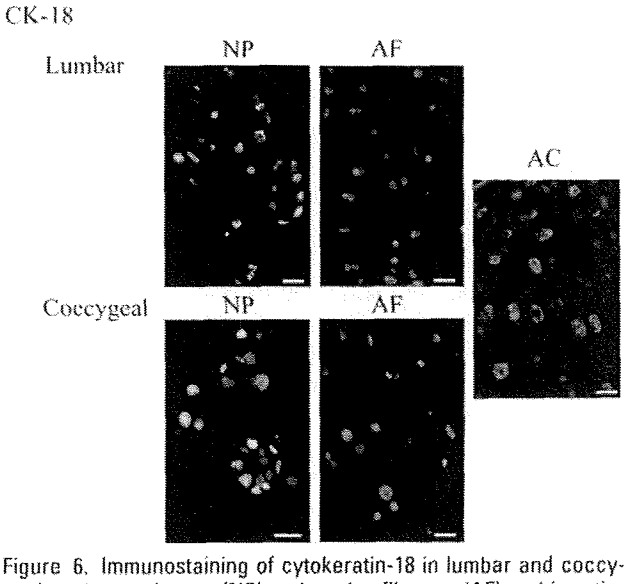


Figure 6. Immunostaining of cytokeratin-18 in lumbar and coccygeal nucleus pulposus (NP) and anulus fibrosus (AF) and in articular cartilage (AC) cells. The majority of lumbar and coccygeal NP cells stain strongly positive, whereas AF and AC cell staining is weaker or negative. Scale bars: 100 $\mu$m.

Figure 7. Immunolocalization of glypican-3 in coccygeal anulus fibrosus. Scale bar: 50 μm.

finding confirms some of the limitations of microarrays and corroborates the critical need to validate microarray data by a second methodology such as quantitative real-time RT-PCR.[27,28]

This is the first study reporting on the expression and localization of A2M, DSC2, NCAM1 (CD56), and CK18 in mature NP tissue of a non-notochordal species. Although the functional role of these proteins remains to be elucidated, the considerable differences in tissue distribution suggest that they may have specific physiologic functions in the NP. For instance, A2M is known as a potent protease inhibitor that also inhibits aggrecanases.[29] Therefore, a constitutively increased A2M expression in the NP, which is particularly rich in aggrecan, is of physiologic relevance. Desmocollins belong to a group of cadherins, and DSC2 is recognized as a membrane glycoprotein.[30] NCAM1 (CD56) is involved in contact-mediated cell interactions. Although this molecule is primarily expressed in cells of the nervous system, it has been identified in various tissues during development.[31,32] One major reason why we further examined the latter 2 molecules is that they represent cell surface molecules. In view of potential cell sorting or cell separation procedures, the expression of cell surface or cell adhesion proteins is of particular interest. Immunohistochemistry shows that both DSC2 and NCAM1 (CD56) are expressed in NP but not in AF cells, but a potential use of these proteins to identify NP cells requires further investigation. Given that DSC2 is expressed also in AC, it could, however, not separate NP from AC cells. Cytokeratin 18 has been identified in human notochordal cells during development.[33,34] Interestingly, remnants of cytokeratin-positive cells were also found in normal adult NP, although the expression of such simple epithelial cytokeratins has generally been associated with classic chordomas.[33,35]

Of the 5 genes that had shown significant expression differences between NP and AC in the rat only 2 demonstrated a similar pattern in the dog. In agreement with the rat results, both COMP and MGP expression were lower in NP than in AC also in the dog. In contrast, GPC3, which had been proposed as an NP marker in the rat, displayed no difference in the expression between NP and AC, but was enhanced in AF. Higher expression of GPC3 in AF compared to AC had already been observed in mature rats. Recently, it was reported that during human development, GPC3 was expressed in a highly tissue- and stage-specific manner.[36] Hence, the substantial discrepancy between rat and dog NP might be related to differences in the development of the NP tissues. Moreover, PTN also showed an opposite trend in the dog compared to the rat, with higher expression levels in AC than in NP and AF. Hence, findings from one species may or may not apply to another species and need to be confirmed for a specific molecule or situation. The observed differences may partly be related to the fact that rat discs are considered as notochordal, whereas discs from the beagle dogs are non-notochordal.[2,3]

Caudal discs are frequently used in animal models. Although similarities in biochemical and biomechanical properties have been found among species and between caudal and lumbar discs,[37,38] the limitations of the use of caudal discs need to be taken into consideration.[39] With respect to the genes and proteins investigated in this study, the general expression pattern was similar in lumbar and caudal discs. Nevertheless, certain variations such as the enhanced gene expression of NCAM1 (CD56) in the caudal NP, that was confirmed at the protein level, and of PTN and VIM in the caudal AF are evident.

In conclusion, this study reports on the expression of distinct molecules that have not been described previously in the IVD, in non-notochordal discs comparable with human discs. Tissue-specific differences in expression profiles may qualify some molecules as markers, although further studies will be required. In particular, considerable interspecies differences were noted when comparing rat and dog tissues, whereas the variations between disc levels (caudal *vs.* lumbar) were less significant. It might be speculated that the NP phenotype of the beagle as a chondrodystrophoid dog breed is more similar to the human than the NP of species whose discs do not naturally degenerate; however, a comparison with human IVD will be necessary to confirm this statement with respect to the expression profile of specific genes and proteins. Finally, while the present study only addressed normal disc gene expression profiles, there is also a need for comparing profiles between healthy and degenerated discs. Nevertheless, in view of the limited availability of healthy human IVD tissues, studies on species with similar characteristics – such as chondrodystrophoid dogs – largely contribute to a better understanding of the IVD and its relevant cell types. This

knowledge is of substantial value for the development of new treatment strategies for IVD diseases.

## ■ Key Points

- Phenotypic differences between dog nucleus pulposus and anulus fibrosus were investigated by large scale gene expression profiling.
- Variations were noted in relative expression levels between lumbar and coccygeal discs.
- Immunohistochemistry confirmed gene expression differences at the protein level.
- There were considerable divergences comparing rat and non-notochordal dog discs that are more similar to human discs.

## References


1. Luoma K, Riihimaki H, Luukkonen R, Raininko R, et al. Low back pain in relation to lumbar disc degeneration. *Spine* 2000;25:487–92.
2. Boden SD, Davis DO, Dina TS, et al. Abnormal magnetic-resonance scans of the lumbar spine in asymptomatic subjects. A prospective investigation. *J Bone Joint Surg Am* 1990;72:403–8.
3. Boos N, Weissbach S, Rohrbach H, et al. Classification of age-related changes in lumbar intervertebral discs: 2002 Volvo Award in basic science. *Spine* 2002;27:2631–44.
4. Miller JA, Schmatz C, Schultz AB. Lumbar disc degeneration: correlation with age, sex, and spine level in 600 autopsy specimens. *Spine* 1988;13:173–8.
5. Thompson JP, Oegema TR, Jr., Bradford DS. Stimulation of mature canine intervertebral disc by growth factors. *Spine* 1991;16:253–60.
6. Osada R, Ohshima H, Ishihara H, et al. Autocrine/paracrine mechanism of insulin-like growth factor-1 secretion, and the effect of insulin-like growth factor-1 on proteoglycan synthesis in bovine intervertebral discs. *J Orthop Res* 1996;14:690–9.
7. Takegami K, Thonar EJ, An HS, et al. Osteogenic protein-1 enhances matrix replenishment by intervertebral disc cells previously exposed to interleukin-1. *Spine* 2002;27:1318–25.
8. Nishida K, Kang JD, Gilbertson LG, et al. Modulation of the biologic activity of the rabbit intervertebral disc by gene therapy: an in vivo study of adenovirus-mediated transfer of the human transforming growth factor beta 1 encoding gene. *Spine* 1999;24:2419–25.
9. Trout JJ, Buckwalter JA, Moore KC. Ultrastructure of the human intervertebral disc: II. Cells of the nucleus pulposus. *Anat Rec* 1982;204:307–14.
10. Sakai D, Mochida J, Yamamoto Y, et al. Transplantation of mesenchymal stem cells embedded in Atelocollagen gel to the intervertebral disc: a potential therapeutic model for disc degeneration. *Biomaterials* 2003;24:3531–41.
11. Sakai D, Mochida J, Iwashina T, et al. Differentiation of mesenchymal stem cells transplanted to a rabbit degenerative disc model: potential and limitations for stem cell therapy in disc regeneration. *Spine* 2005;30:2379–87.
12. Sakai D, Mochida J, Iwashina T, et al. Regenerative effects of transplanting mesenchymal stem cells embedded in atelocollagen to the degenerated intervertebral disc. *Biomaterials* 2006;27:335–45.
13. Risbud MV, Albert TJ, Guttapalli A, et al. Differentiation of mesenchymal stem cells towards a nucleus pulposus-like phenotype in vitro: implications for cell-based transplantation therapy. *Spine* 2004;29:2627–32.
14. Steck E, Bertram H, Abel R, et al. Induction of intervertebral disc-like cells from adult mesenchymal stem cells. *Stem Cells* 2005;23:403–11.
15. Richardson SM, Walker RV, Parker S, et al. Intervertebral disc cell-mediated mesenchymal stem cell differentiation. *Stem Cells* 2006;24:707–16.
16. Lee CR, Sakai D, Nakai T, et al. A phenotypic comparison of intervertebral disc and articular cartilage cells in the rat. *Eur Spine J* 2007;16:2174–85.
17. Alini M, Eisenstein SM, Ito K, et al. Are animal models useful for studying human disc disorders/degeneration? *Eur Spine J* 2008;17:2–19.
18. Burton-Wurster N, Mateescu RG, Todhunter RJ, et al. Genes in canine articular cartilage that respond to mechanical injury; gene expression studies with Affymetrix canine GeneChip. *J Hered* 2005;96:821–8.
19. Cardin S, Libby E, Pelletier P, et al. Contrasting gene expression profiles in two canine models of atrial fibrillation. *Circ Res* 2007;100:425–33.
20. Reno C, Marchuk L, Sciore P, et al. Rapid isolation of total RNA from small samples of hypocellular, dense connective tissues. *Biotechniques* 1997;22:1082–6.
21. Poiraudeau S, Monteiro I, Anract P, et al. Phenotypic characteristics of rabbit intervertebral disc cells. Comparison with cartilage cells from the same animals. *Spine* 1999;24:837–44.
22. Horner HA, Roberts S, Bielby RC, et al. Cells from different regions of the intervertebral disc: effect of culture system on matrix expression and cell phenotype. *Spine* 2002;27:1018–28.
23. Hunter CJ, Matyas JR, Duncan NA. Cytomorphology of notochordal and chondrocytic cells from the nucleus pulposus: a species comparison. *J Anat* 2004;205:357–62.
24. Trout JJ, Buckwalter JA, Moore KC, et al. Ultrastructure of the human intervertebral disc. I. Changes in notochordal cells with age. *Tissue Cell* 1982;14:359–69.
25. Jovanovic BD, Bergan RC, Kibbe WA. Some aspects of analysis of gene array data. *Cancer Treat Res* 2002;113:71–89.
26. Wang Y, Barbacioru C, Hyland F, et al. Large scale real-time PCR validation on gene expression measurements from two commercial long-oligonucleotide microarrays. *BMC Genomics* 2006;7:59.
27. Chuaqui RF, Bonner RF, Best CJ, et al. Post-analysis follow-up and validation of microarray experiments. *Nat Genet* 2002;32(suppl):509–14.
28. Rajeevan MS, Vernon SD, Taysavang N, et al. Validation of array-based gene expression profiles by real-time (kinetic) RT-PCR. *J Mol Diagn* 2001;3:26–31.
29. Tortorella MD, Arner EC, Hills R, et al. Alpha2-macroglobulin is a novel substrate for ADAMTS-4 and ADAMTS-5 and represents an endogenous inhibitor of these enzymes. *J Biol Chem* 2004;279:17554–61.
30. Kowalczyk AP, Borgwardt JE, Green KJ. Analysis of desmosomal cadherin-adhesive function and stoichiometry of desmosomal cadherin-plakoglobin complexes. *J Invest Dermatol* 1996;107:293–300.
31. Rutishauser U, Acheson A, Hall AK, et al. The neural cell adhesion molecule (NCAM) as a regulator of cell-cell interactions. *Science* 1988;240:53–7.
32. Rutishauser U. NCAM and its polysialic acid moiety: a mechanism for pull/push regulation of cell interactions during development? *Dev Suppl* 1992;99–104.
33. Stosiek P, Kasper M, Karsten U. Expression of cytokeratin and vimentin in nucleus pulposus cells. *Differentiation* 1988;39:78–81.
34. Gotz W, Kasper M, Fischer G, et al. Intermediate filament typing of the human embryonic and fetal notochord. *Cell Tissue Res* 1995;280:455–62.
35. Heikinheimo K, Persson S, Kindblom LG, et al. Expression of different cytokeratin subclasses in human chordoma. *J Pathol* 1991;164:145–50.
36. Iglesias BV, Centeno G, Pascuccelli H, et al. Expression pattern of glypican-3 (GPC3) during human embryonic and fetal development. *Histol Histopathol* 2008;23:1333–40.
37. Oshima H, Ishihara H, Urban JP, et al. The use of coccygeal discs to study intervertebral disc metabolism. *J Orthop Res* 1993;11:332–8.
38. Beckstein JC, Sen S, Schaer TP, et al. Comparison of animal discs used in disc research to human lumbar disc: axial compression mechanics and glycosaminoglycan content. *Spine* 2008;33:E166–73.
39. Demers CN, Antoniou J, Mwale F. Value and limitations of using the bovine tail as a model for the human lumbar spine. *Spine* 2004;29:2793–9.

*Osteoarthritis and Cartilage* (2010) **18**, 416–423

doi:10.1016/j.joca.2009.09.009

**Osteoarthritis and Cartilage**

OA OSTEOARTHRITIS

# Variations in gene and protein expression in human nucleus pulposus in comparison with annulus fibrosus and cartilage cells: potential associations with aging and degeneration

J. Rutges†, L. B. Creemers†, W. Dhert†, S. Milz‡, D. Sakai§, J. Mochida§, M. Alini‡ and S. Grad‡*

† *Department of Orthopaedics, University Medical Center, Utrecht, The Netherlands*

‡ *AO Research Institute, Davos, Switzerland*

§ *Department of Orthopaedic Surgery, Surgical Science, Tokai University School of Medicine, Kanagawa, Japan*

## Summary

*Objective*: Regardless of recent progress in the elucidation of intervertebral disc (IVD) degeneration, the basic molecular characteristics that define a healthy human IVD are largely unknown. Although work in different animal species revealed distinct molecules that might be used as characteristic markers for IVD or specifically nucleus pulposus (NP) cells, the validity of these markers for characterization of human IVD cells remains unknown.

*Design*: Eleven potential marker molecules were characterized with respect to their occurrence in human IVD cells. Gene expression levels of NP were compared with annulus fibrosus (AF) and articular cartilage (AC) cells, and potential correlations with aging were assessed.

*Results*: Higher mRNA levels of cytokeratin-19 (KRT19) and of neural cell adhesion molecule-1 were noted in NP compared to AF and AC cells. Compared to NP cytokeratin-18 expression was lower in AC, and alpha-2-macroglobulin and desmocollin-2 lower in AF. Cartilage oligomeric matrix protein (COMP) and glypican-3 expression was higher in AF, while COMP, matrix gla protein (MGP) and pleiotrophin expression was higher in AC cells. Furthermore, an age-related decrease in KRT19 and increase in MGP expression were observed in NP cells. The age-dependent expression pattern of KRT19 was confirmed by immunohistochemistry, showing the most prominent KRT19 immunoreaction in the notochordal-like cells in juvenile NP, whereas MGP immunoreactivity was not restricted to NP cells and was found in all age groups.

*Conclusions*: The gene expression of KRT19 has the potential to characterize human NP cells, whereas MGP cannot serve as a characteristic marker. KRT19 protein expression was only detected in NP cells of donors younger than 54 years.


*Key words*: Intervertebral disc cells, Phenotype expression, Nucleus pulposus, Annulus fibrosus, Articular cartilage, Human, Aging.

## Introduction

Degeneration of the intervertebral disc (IVD) and related spinal disorders are leading causes of morbidity, resulting in substantial pain, disability and increased health care costs[1]. The IVD comprises the highly hydrated nucleus pulposus (NP), the surrounding multilaminar annulus fibrosus (AF) and the cartilaginous endplates. Pathophysiological evidence indicates that IVD degeneration starts in the NP, where the concentration of proteoglycans and the synthesis of type II collagen decrease[2,3]. At the same time denaturation of type II collagen fibers and synthesis of type I collagen occurs[3]. As a consequence the NP loses its osmotic properties and becomes fibrotic; the disc loses its ability to transmit intervertebral forces and further degenerative processes may occur.

Regeneration of NP tissue in the early stages of degeneration may slow down or even reverse the degenerative processes and might possibly restore part of the degenerated disc. Thus, regenerative medicine and biological therapies hold great promise. In particular the therapeutic implications of stem cells have been highly anticipated by both the clinical and scientific communities[4,5]. The challenge in characterizing cellular degeneration and ultimately accomplishing cellular regeneration begins with the identification of the molecular phenotype of the cells that constitute the NP. The NP includes small cells commonly referred to as "chondrocyte-like", since they have a similar rounded morphology and synthesize similar extracellular matrix macromolecules as articular chondrocytes. Currently, no reliable markers exist to distinguish NP cells from the chondrocytes from hyaline cartilage. A cell population with the properties of articular cartilage (AC) would fail to restore the necessary function of the IVD because the requisite fluid properties unique to the IVD would not be recreated. While the ratio of proteoglycan to collagen shows a certain potential to separate disc cells, recent research has focused on the clarification of their molecular phenotype[6]. In a recent study, rat NP cells were compared with cells from the AF and AC tissues by means of large scale microarray gene expression screening. Subsequent quantitative gene expression and immunohistochemical analyses identified distinct molecules, namely glypican-3 (GPC3) and cytokeratin-19

*Address correspondence and reprint requests to: Sibylle Grad, AO Research Institute, Clavadelerstrasse 8, 7270 Davos, Switzerland. Tel: 41-81-414-24 80; Fax: 41-81-414-22-88; E-mail: sibylle.grad@aofoundation.org

Received 18 March 2009; revision accepted 27 September 2009.

(KRT19), as promising candidates for NP cell characterization[7]. Similar studies in the beagle dog revealed additional potential NP marker molecules, including alpha-2-macroglobulin (A2M), cytokeratin-18 (KRT18), desmocollin-2 (DSC2), and neural cell adhesion molecule-1 (NCAM1)[8].

However, considerable developmental, anatomical, and biochemical differences among species are likely to affect the phenotypical characteristics of the disc cells[9]. In particular the presence of notochordal cells, which are regarded to be remnants of the embryonic notochord, in the NP is the cause of substantial inter-species variation. Mice, rats, rabbits, and non-chondrodystrophoid dogs retain a predominantly notochordal NP until adulthood and often throughout life, whereas bovine, ovine and chondrodystrophoid dogs closer resemble humans in that the number of notochordal cells rapidly decreases after birth[10]. Moreover, differences in tissue size, oxygen and nutrient supply, and biomechanical requirements are also likely to affect the molecular features of the cells in the disc. As a consequence, observations from animal discs will not necessarily apply to human discs. Nevertheless, animal studies are indispensable for screening purposes, since they allow investigation of normal healthy tissues with larger sample size and smaller inter-individual variability. Due to the limited availability of healthy and viable human IVD tissue, comprehensive screening is difficult in human individuals. The aim of this study therefore was to evaluate the presence and distribution of the molecules that were found to be differently expressed in disc and cartilage cell populations in various animal species in human disc cells. To account for potential variations related to aging and degeneration, cell and tissue samples from individuals of different age groups and disc degeneration grades were examined.

## Materials and methods

### ISOLATION OF NP, AF, AND AC CELLS

The study was approved by the medical ethical committee of the University Medical Center (UMC) Utrecht and the scientific committee from the Department of Pathology of the UMC Utrecht. Eleven patients with no known history of IVD disease were included in the study. Samples were obtained within an average of 17.5 h after death of the patient (range 6.25–23.0 h). The age of the individuals ranged from 22 to 81 years (average 46 ± 20 years; median 43 years), and the average degree of disc degeneration, assessed according to the Thompson score[11], was 2.2 ± 1.0 (median 2) (Table I). IVD tissue was harvested from segments between L1 and L5 and was separated into NP and AF tissue. To exclude any contamination by AF tissue, only the innermost part of the disc was harvested to be assigned to NP tissue, whereas the transition zone, including part of the inner AF, was entirely excluded from analysis. This is of particular importance for aged discs, where it can be difficult to clearly distinguish NP and AF tissues. AC was harvested from the patellae of the same patients. Chondrocytes were extracted from full thickness cartilage which implies mixed populations of superficial, middle and deep zone cells. Gene expression data thus represent an average cellular expression of target mRNA.

Tissue was cut into small pieces and cells were enzymatically isolated using sequential pronase (Roche) and type II collagenase (Worthington Biochemical) digestion with DNase II (Sigma) added to prevent cell clumping. AC and AF were treated with 0.2% pronase/0.004% DNase for 1 h, then with 200 U/mL collagenase/0.004% DNase over night. NP was treated with 0.2% pronase/0.004% DNase for 1 h, then with 100 U/mL collagenase/0.004% DNase for 8 h, stirring at 37°C in humidified atmosphere. After enzymatic isolation cell suspensions were filtered through a 70 μm cell strainer, washed twice with Dulbecco's Modified Eagles Medium, and lysed in TRI Reagent (Molecular Research Center, Cincinnati, OH). Samples were stored at −80°C until RNA isolation.

Table I

*Patients included for gene expression analysis of NP, AF, and AC cells. IVD tissue was harvested from discs between L1 and L5 and separated in NP and AF; AC was harvested from the patella joint surface. Cartilage quality was macroscopically assessed and was without detectable changes for patients 1–9. Slight degenerative changes were detected in patient 10, and signs of osteoarthritis in patient 11*

| Patient number | Age | Gender | Thompson grade |
|---|---|---|---|
| 1 | 22 | M | 1 |
| 2 | 25 | M | 1 |
| 3 | 25 | M | 1 |
| 4 | 32 | M | 1–2 |
| 5 | 40 | M | 2 |
| 6 | 43 | M | 2 |
| 7 | 46 | M | 2–3 |
| 8 | 56 | M | 3 |
| 9 | 61 | F | 3 |
| 10 | 72 | M | 4 |
| 11 | 81 | F | 3 |

### RNA EXTRACTION AND REAL TIME RT-PCR

RNA was isolated using a modified TriSpin method[7,12]. Briefly, bromochloro-propane (Sigma) was added to the lysate, phases were separated, and ethanol (Merck) added to the aqueous phase. Total RNA was extracted using the SV Total RNA Isolation System (Promega), which includes an on-column DNAse digestion, and eluted in 100 μl of RNase-free water. TaqMan reverse transcription reagents (Applied Biosystems, Foster City, CA) were used for cDNA synthesis. PCR was performed with an SDS 7500 real time PCR instrument using TaqMan Gene Expression Master Mix (all from Applied Biosystems) and standard thermal conditions (10 min 95°C for polymerase activation, followed by 45 cycles of 95°C for 15 s and 60°C for 60 s). Primer-probe systems, purchased as Gene Expression Assays, were from Applied Biosystems. Genes that were previously found to be differentially expressed in NP compared to AF and/or AC cells in the rat and/or chondrodystrophoid dog were chosen for analysis (Table II)[7,8,13]. Expression of target genes was normalized to the 18S ribosomal RNA as the endogenous control. Relative mRNA levels were calculated according to the 2^(delta Ct) method and presented as log(2) transformed values[14,15].

### IMMUNOHISTOCHEMISTRY

For histological analysis human IVD tissue was obtained as part of a standard postmortem procedure, in which a section of the lumbar and thoracic spine is removed for diagnostic purposes. IVD samples were stored in the UMC Utrecht Biobank of the Department of Pathology. Collection and analysis of the IVDs was approved by the medical ethical committee of the UMC Utrecht and the scientific committee of the Department of Pathology of the UMC Utrecht. Samples were obtained within a mean of 17.7 h after death of the patient, 95% within 24 h after death. Between death and tissue collection the deceased patients were kept at the mortuary at 4°C. From all patients the IVD between the fourth and fifth lumbar vertebra (spinal motion segment L4–L5), including the adjacent endplates, was obtained. The grade of degeneration was scored by three individual observers using the classification of Thompson *et al.*[11]. After individual scoring the values were averaged; outliers, i.e., differences of more than 1 Thompson grade, were re-evaluated by the three observers at a consensus meeting.

The expression and localization of KRT19 and matrix gla protein (MGP) in IVD tissue was evaluated in 41 human individuals aged between 3 and 86 years (average 47 ± 25 years; median 51 years, Table III). Sagittal slices of the motion segments were fixed in formalin, decalcified with Kristensen's solution (50% formic acid and 68 g/L sodium formiate) in a microwave at

Table II

*Gene expression assays used for real time PCR (from Applied Biosystems)*

| Gene | Assay code |
|---|---|
| A2M | Hs_00163474_m1 |
| CD24 | Hs_00273561_s1 |
| COMP | Hs_00164359_m1 |
| DSC2 | Hs_00245200_m1 |
| GPC3 | Hs_00170471_m1 |
| KRT18 | Hs_01920599_gH |
| KRT19 | Hs_00761767_s1 |
| MGP | Hs_00179899_m1 |
| NCAM1 | Hs_00169851_m1 |
| PTN | Hs_00383235_m1 |
| VIM | Hs_00185584_m1 |

Table III

*Immunohistochemical results obtained from IVD sections from the UMC Utrecht Biobank of the Dept. of Pathology. Only discs between the fourth and fifth human lumbar vertebra (L4–L5) were assessed. Cells were classified according to their topographical position within the disc tissue*

| Patient number | Age | Gender | Thompson grade | KRT19 | MGP | | | | |
|---|---|---|---|---|---|---|---|---|---|
| | | | | NP | NP | IAF | OAF | EP | AOA |
| 1 | 3 | F | 1 | ++ | +++ | – | – | – | ++ |
| 2 | 3 | F | 1 | +++ | N/A | N/A | N/A | N/A | N/A |
| 3 | 6 | F | 1 | – | +++ | ++ | ++ | – | N/A |
| 4 | 14 | M | 1 | +++ | +++ | ++ | +++ | – | +++ |
| 5 | 14 | F | 1 | ++ | +++ | +++ | +++ | – | N/A |
| 6 | 14 | F | 1 | – | – | – | ++ | – | N/A |
| 7 | 17 | M | 2 | +++ | +++ | – | – | – | +++ |
| 8 | 18 | M | 1 | + | – | – | – | N/A | N/A |
| 9 | 19 | F | 1 | – | +++ | ++ | ++ | – | +++ |
| 10 | 21 | M | 1 | ++ | +++ | + | ++ | – | +++ |
| 11 | 22 | F | 1 | + | ++ | – | N/A | – | N/A |
| 12 | 25 | M | 1 | – | ++ | – | – | – | ++ |
| 13 | 35 | F | 2 | +++ | ++ | +++ | +++ | – | +++ |
| 14 | 35 | M | N/A | – | +++ | ++ | ++ | – | +++ |
| 15 | 36 | M | 2 | – | ++ | + | + | – | N/A |
| 16 | 38 | M | 2 | – | + | – | – | – | + |
| 17 | 41 | M | 2 | (+) | +++ | + | +++ | – | +++ |
| 18 | 44 | M | 2 | – | – | – | – | – | – |
| 19 | 47 | F | 3 | – | ++ | – | – | – | – |
| 20 | 51 | F | 2 | – | (+) | – | + | – | +++ |
| 21 | 51 | F | 2 | (+) | ++ | – | – | – | + |
| 22 | 54 | F | 4 | (+) | +++ | – | +++ | – | N/A |
| 23 | 57 | M | 4 | – | ++ | ++ | +++ | – | N/A |
| 24 | 59 | M | 4 | – | +++ | ++ | N/A | – | N/A |
| 25 | 60 | M | 5 | – | +++ | ++ | ++ | – | +++ |
| 26 | 62 | F | 2 | – | – | – | – | – | +++ |
| 27 | 62 | M | 5 | – | +++ | +++ | +++ | – | +++ |
| 28 | 63 | M | 3 | – | ++ | + | – | – | N/A |
| 29 | 67 | F | 5 | – | + | N/A | N/A | N/A | N/A |
| 30 | 68 | F | 5 | – | N/A | N/A | N/A | + | ++ |
| 31 | 70 | M | 4 | – | ++ | – | – | – | ++ |
| 32 | 71 | M | 3 | – | ++ | – | – | N/A | NA |
| 33 | 72 | M | N/A | – (*) | (+) | – | – | – | NA |
| 34 | 72 | M | 5 | – | +++ | – | +++ | + | +++ |
| 35 | 73 | F | 3 | – | +++ | +++ | – | – | N/A |
| 36 | 74 | F | 3 | – | ++ | – | – | – | +++ |
| 37 | 76 | M | 3 | – | ++ | +++ | – | – | +++ |
| 38 | 76 | F | 5 | – | + | (+) | – | – | +++ |
| 39 | 80 | F | 5 | – (*) | +++ | ++ | N/A | N/A | +++ |
| 40 | 82 | F | 4 | – | ++ | – | – | – | N/A |
| 41 | 86 | F | 4 | – | + | – | – | – | N/A |

Grading scheme: (+) = 1–2 positive cells; + = 3–4 positive cells; ++ = 5–10 positive cells; +++ = >10 positive cells per field of view. For analysis a Zeiss Axioplan2 microscope equipped with a 20× objective (Neofluar) and a 10× ocular was used. IAF: Inner annulus fibrosus; OAF: Outer annulus fibrosus; EP: Cartilaginous endplate; AOA: Attachment of outer annulus fibrosus; N/A: not available. KRT19 positive cells were only detected in the NP and in 2 cases of severe degenerative disc changes in the EP (*).

150 W and 50°C for 6 h, dehydrated in graded ethanol series, and embedded in paraffin[16]. Sections were deparaffinized, treated with 3% hydrogen peroxide in methanol for 30 min and then with heated (95°C) citrate buffer (10 mM sodium citrate, 0.05% Tween20, pH 6.0) for 20 min for antigen retrieval. Then they were blocked with 5% normal horse serum for 1 h, and were incubated with mouse monoclonal anti-KRT19 antibody (clone A53-B/A2; cat. no. EXB-11-120, Exbio, Praha, CZ) or mouse monoclonal anti-MGP antibody (clone 52.1C5D; cat. no. ALX-804-512, Alexis Biochemicals, Lausen, CH) at a concentration of 5 µg/ml over night at 4°C. Negative control sections were incubated without primary antibody. Biotinylated secondary anti-mouse antibody (dilution 1:200; Vectastain ABC-kit *Elite*, cat. no. PK-6102, Vector Laboratories, Burlingame, USA) was applied, followed by ABC complex, and chromogen development using diaminobenzidine (DAB Kit, cat. no. SK-4100, Vector Laboratories, Burlingame, USA). Sections were counterstained with Mayer's haematoxylin.

### STATISTICAL ANALYSIS

Differences in relative gene expression levels between paired NP and AF and paired NP and AC were assessed by the Wilcoxon Signed Ranks test. Correlations between relative gene expression and age or disc degeneration grade were determined using the Pearson correlation analysis. $P < 0.05$ was considered as significant.

## Results

### GENE EXPRESSION

In both the NP vs AF and the NP vs AC comparisons, pronounced gene expression differences were observed for KRT19. Levels of KRT19 mRNA were constantly higher in the NP than in both AF and AC cells, although the extent of up-regulation varied between individuals. NCAM1 expression was also increased in NP compared to AF and AC cells, while the expression of A2M and DSC2 was higher in NP than in AF cells and KRT18 expression was higher in NP than in AC cells. On the other hand, mRNA

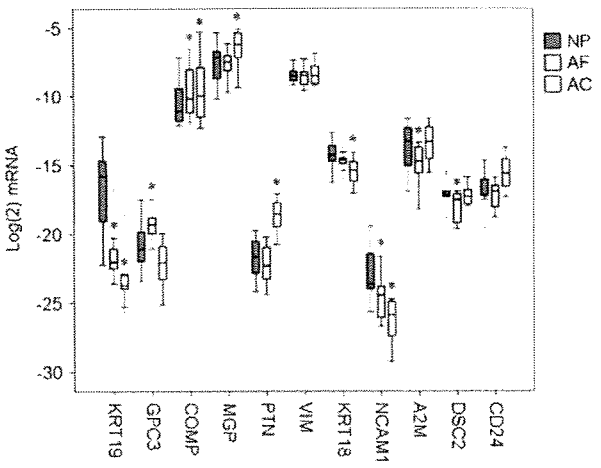


Fig. 1. Relative mRNA expression in human NP, AF, and AC cells. Expression levels were normalized to 18S rRNA as the endogenous control. *$P < 0.05$ in pair-wise comparison of NP with corresponding AF or AC; N = 9–11.

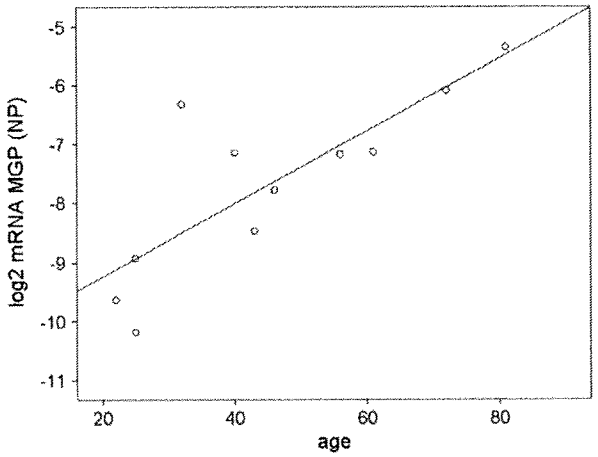


Fig. 3. Relative mRNA expression for MGP in NP cells of 11 individuals between 22 and 81 years of age. Gene expression was normalized to the 18S ribosomal RNA. An increase in the MGP expression level with increasing age is noted.

expression levels of GPC3 and cartilage oligomeric matrix protein (COMP) were higher in the AF compared to the NP, whereas COMP, MGP, and pleiotrophin (PTN) were expressed more highly in the AC than in the NP cells. No differences in vimentin (VIM) and Cluster of Differentiation 24 antigen (CD24) expression were noted between NP and AF or AC cells (Fig. 1).

While the KRT19 expression of AC and AF cells did not change throughout age groups, its expression in the NP cells showed a decrease with age ($P = 0.032$; Fig. 2). However, in spite of this decrease, KRT19 was still more highly expressed in the NP compared to the AF and AC cells even in older individuals. A correlation between age and gene expression in NP cells was also found for MGP mRNA, which increased with increasing age ($P = 0.003$; Fig. 3). In the AF cells, increasing levels of PTN mRNA were noted with aging ($P = 0.023$; data not shown). The expression of MGP in NP cells was also positively correlated with the degree of degeneration ($P = 0.007$). The relation between KRT19 level in the NP and degeneration grade was found to be almost significant ($P = 0.061$). No association between age or degeneration grade and the level of expression was detected with any of the other genes analysed. However, in agreement with previous reports, there was a strong relationship between age and degeneration grade of the disc ($P < 0.001$).

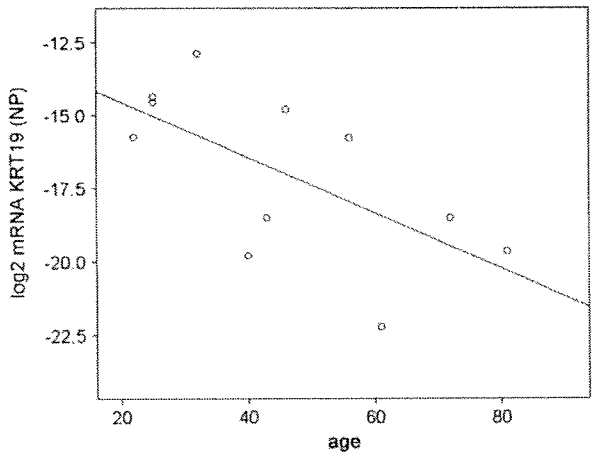


Fig. 2. Relative mRNA expression for KRT19 in NP cells of 11 individuals between 22 and 81 years of age. Gene expression was normalized to the 18S ribosomal RNA. A decrease in the KRT19 expression level with increasing age is noted.

### IMMUNOHISTOCHEMISTRY

KRT19 was chosen for immunohistochemical analysis, since this molecule showed most pronounced differences between NP and AF or AC with respect to mRNA expression, whereas MGP was selected for analysis at the protein level because of its apparent age- and degeneration-dependent increase in the NP cells, which are of main interest in this study.

In the NP of juvenile discs (<5 years of age), clusters of large cells with a notochordal morphology were identified. These cells were positive for KRT19 [Fig. 4(A)], while neither cells within the AF nor cells of the cartilaginous endplate revealed any positive labelling [Fig. 4(B), Table III]. In the NP of young discs with Thompson score 1 but without apparent existence of notochordal cells (age range 6–25 years), KRT19 positive cells were observed in 60% ($n = 6/10$) of the individuals. Labelling was located predominantly intracellular and was limited to a small number of cells that had a somewhat chondrocytic appearance with no morphological evidence of a notochordal cell phenotype [Fig. 4(C, D)]. On the other hand, the majority of healthy adult discs did not reveal any immunoreactivity for KRT19 [Fig. 4(E)]. In two degenerate discs however (patients with sepsis), positive cells were detected adjacent to fissures associated with degenerative changes of the cartilaginous endplate [Fig. 4(G)]. These cells exhibited a characteristic chondrocyte-like morphology, were located at the border between cartilaginous endplate and NP and were not regarded as NP cells.

The number of MGP positive cells in general was higher than the number of KRT19 positive cells, but non labelled

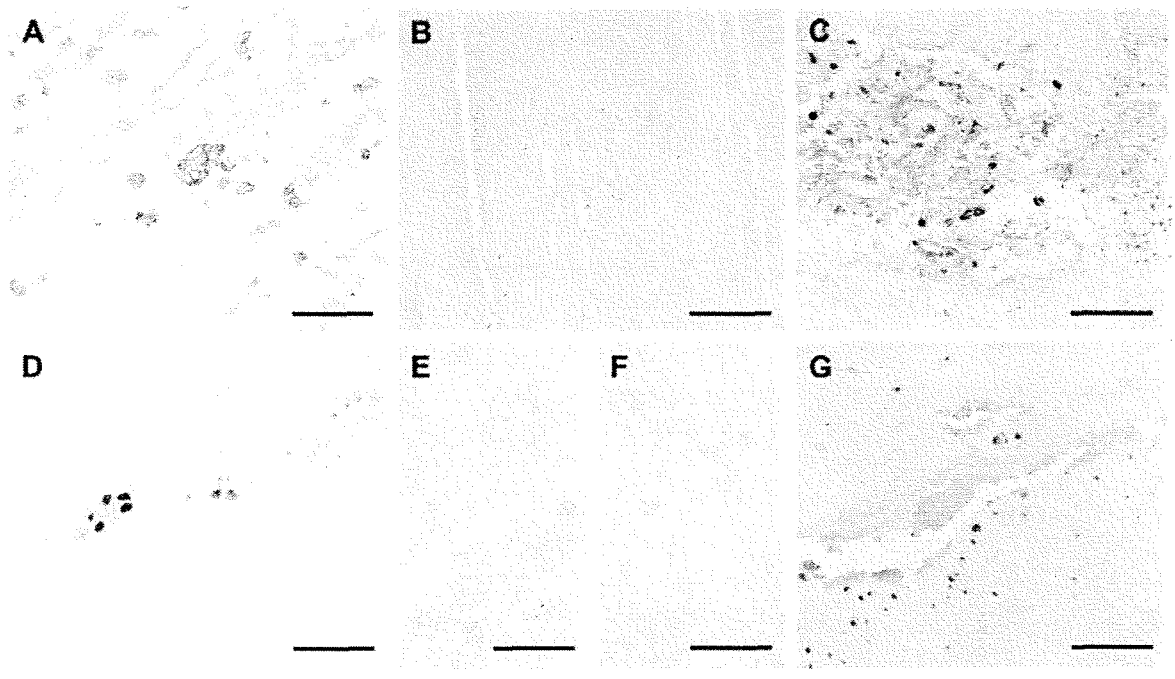


Fig. 4. Immunolabelling characteristics for KRT19. (A) Cells within the NP of a 3-year-old human female label positive for KRT19. (B) No KRT19 positive cells are detected in the inner annulus of a 21-year-old male individual. (C) A group of KRT19 positive cells in the NP of a 14-year-old male. (D) Small group of KRT19 positive cells from the NP of a 21-year-old male (same individual as in B). (E) NP of a 47-year-old female with Thompson grade 3. No positive labelling can be detected. (F) Control from same individual as in E. (G) 72-year-old male donor with disc degeneration grade 4. The image shows the edge of the NP region. The cartilaginous endplate is at the bottom of the image. Several KRT19 positive cells with a chondrocyte-like morphology can be detected. All scale bars = 100 μm.

cells clearly constitute the largest cell fraction. However, in juvenile and young adult discs positive cells could be detected in the NP (Table III). MGP positive cells were found in distinct clusters of NP cells in young individuals [Fig. 5(A, B)]. In older more degenerated discs (grade 3 and higher) positive cells were found adjacent to clefts and cracks [Fig. 5(D)]. Furthermore, the outer AF was often immunopositive [Fig. 5(E)], with a decreasing intensity towards the inner AF [Fig. 5(F)]. Labelling was limited to the cells and to a very small portion of the pericellular matrix in their immediate vicinity. The cells and extracellular matrix of the mineralized cartilage of the endplate often demonstrated a positive reaction for MGP, especially at the tidemark [Fig. 5(G, H)]. The non-mineralized cartilage of the endplate was always negative [Fig. 5(G, H)]. The fibrocartilaginous attachment of the outer AF frequently labelled positive [Fig. 5(I)].

## Discussion

Degenerative changes occurring in the IVD have been extensively described and mechanisms, including genetic variations that may cause a predisposition to IVD degeneration are being elucidated. However, the molecular profile that characterizes the normal disc, and in particular the NP cell is still unknown. Previous investigations have suggested potential markers for IVD cells and more specifically for NP cells[7,8,13,17]. The present study is a further contribution to the identification of molecules expressed in human disc cells. It was undertaken to validate potential NP marker molecules identified by large scale gene expression screening in the rat and dog for their potential use with human cells.

Looking at genes previously identified as markers for the rat NP, the expression of KRT19 could be confirmed for human cells. However, a decrease in KRT19 expression with age was noted in the NP, while the expression in AF and AC remained constant. As KRT19 has also been associated with notochordal cells and chordoma, its expression in healthy adult human NP cells may be unexpected[18,19]. Indeed, immunohistochemical analysis confirmed its presence in cells with a notochordal phenotype and further supported the suggestion of an age-dependent expression pattern. At the protein level, KRT19 was barely detectable in the NP after the third decade, although mRNA expression was still clearly measurable. Possible explanations for this finding may include differences in the detection limit between mRNA and protein expression, instability of the mRNA, short protein half-life, or inhibition at the translational level.

In contrast to KRT19, the expression pattern of the other genes that had been found to be expressed more highly in the NP than in the AC in rat specimens, including CD24, was not confirmed in human samples[7,13]. However, GPC3 and PTN expression profiles were similar to observations in beagle dogs[8]. This might be related to the comparable development of the NP with respect to cell phenotype in human individuals and chondrodystrophoid dogs, which clearly differs from the development in rats. Looking at the genes evaluated for the beagle dog, the human samples generally showed a similar expression pattern, with higher levels of KRT18, A2M, and NCAM1 in NP vs AF and/or AC. Besides KRT19, only NCAM1 was expressed more

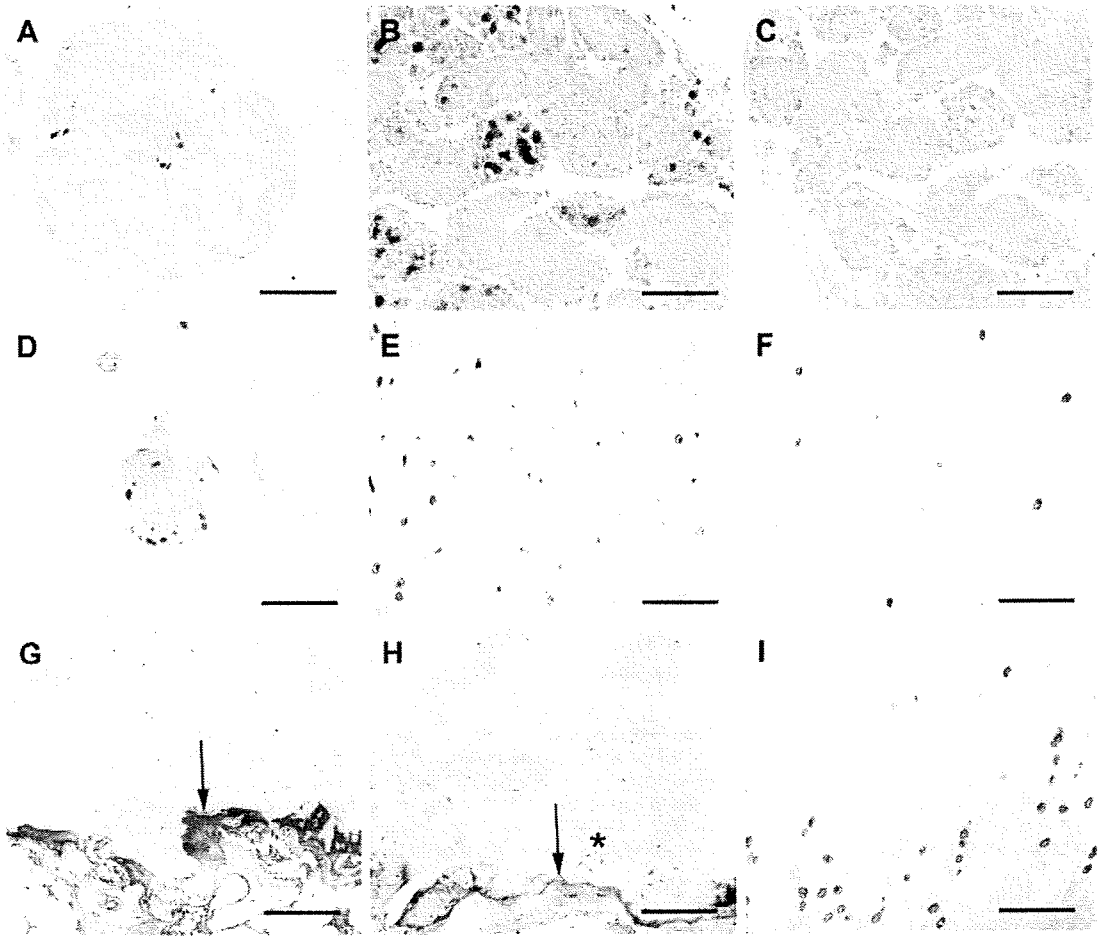


Fig. 5. Immunolabelling characteristics for MGP. (A) Cells within the NP of a 6-year-old human female label positive for MGP. (B) Group of MGP positive cells in the NP of a 17-year-old male. (C) Control from same individual and same region as shown in B. (D) Small group of MGP positive cells from the NP of a 60-year-old male individual with disc degeneration Thompson grade 5. Note that the cells are forming a cluster like structure in the neighbourhood of a fissure. (E) Outer and (F) inner annulus of a 35-year-old female with Thompson grade 2. Several positive cells can be detected. The surrounding extracellular matrix is negative. (G) Endplate cartilage from a 72-year-old male with Thompson grade 5. Note the strong positive labelling at the tidemark (arrow) and in the calcified cartilage. Cells in non-calcified cartilage are all negative. (H) Endplate cartilage from a 35-year-old female individual with Thompson grade 2. The positive labelling at the tidemark (arrow) is clearly visible. Cartilage cells form clusters (*) but are all negative. (I) Fibrocartilaginous attachment of the outer annulus of a 35-year-old female individual (same as in H). The fibrocartilage cells are arranged in characteristic rows and label positive for MGP. Scale bar in G = 200 μm, all other scale bars = 100 μm.

highly in NP than both AF and AC cells in this study. NCAM1 is an integral membrane glycoprotein that can regulate both cell–cell and cell–substrate interactions, primarily through polysialic acid[20,21]. Although it is expressed primarily in the nervous system, NCAM1 has been identified in various tissues in the adult rat[22]. In development NCAM1 plays a significant role in cell differentiation, including diverse functions in osteogenesis and chondrogenesis[23]. However, the fact that NCAM1 was expressed at a low level in all cell types analysed depreciates this molecule as a useful marker for human NP cells.

The matrix protein COMP showed consistently lower expression in NP than in AF and AC cells in all species. This differential expression of COMP in cartilage and disc adds to earlier observations of variations in the relative amounts of distinct matrix molecules in these two tissues[6]. While COMP has been identified and localized in the IVD, its relatively lower expression may reflect differences in the mechanical properties between the NP and cartilage tissues[24]. The main molecular functions of COMP include binding other matrix proteins and catalyzing polymerization of type II collagen fibrils. Furthermore, COMP is reported to prevent vascularization of cartilage and this could also be the case in the IVD tissues[25].

Commonly, work that addresses the disc cell profile leads to the conclusion that disc cells express a predominantly chondrocytic phenotype[26–28]. Investigations on mature bovine IVD cells agreed that NP cells produce more proteoglycans and less collagen than AF and cartilage cells, which is consistent with the higher hydration of the NP tissue[6,29]. In rat spinal units it was demonstrated that NP can be distinguished from adjacent tissues by the expression of proteins that are synthesized in response to restriction in oxygen and nutrient supply[17]. Additional studies in the rat revealed other potentially NP specific markers[7,13]. However, a major disadvantage of using rat NP is the presence of cells with